have revealed that HA positively regulates proliferation, invasion, cell motility, multidrug resistance, and epithelial–mesenchymal transition in many tumor cell lines in vitro and in vivo (reviewed in ref. 23). Furthermore, an HAS inhibitor, 4-methylubelliferon, has been shown to decrease tumor proliferation and metastasis (25, 26).

Despite the importance of HA in tumorigenesis, assessing the role of circulating HA in tumor progression is difficult, because HA administered in the body is rapidly eliminated from the bloodstream (1). In this study, we generated Stab2 KO mice in which plasma HA levels were significantly elevated without any overt phenotype. Unexpectedly, tumor metastasis was markedly suppressed in these mice. We also found that administration of an anti-Stab2 antibody in WT mice elevated circulating HA levels and prevented tumor metastasis. Finally, we found that administration of a high dose of HA prevented the attachment of melanoma cells to the lungs in vivo and in vitro, and examined a possible link between circulating HA levels and tumor metastasis.

Results

Elevation of Circulating HA Levels in Stab2 KO Mice. To address the physiological roles of Stab2 in vivo, we generated a Stab2 KO mouse line by replacing most of the first exon, including the ATG initiation codon and the first intron, with the LacZ and neomycin resistance genes (Figs. S1 *A–C*). The lack of Stab2 expression in KO mice was confirmed by RT-PCR and immunostaining (Figs. S1 *D* and *H* and S2*D*), Stab2-deficient mice were born according to the Mendelian ratio, grew normally, and showed no apparent abnormalities (Fig. S1 *E* and *F*). Histological analyses revealed no significant changes (Fig. S1*G*). Staining of liver sections with the anti-CD31 antibody, which binds HSECs as well as other types of ECs in the liver, demonstrated normal development of HSECs (Fig. S1*H*). Furthermore, we found no significant differences in conventional diagnostic markers for functions of the pancreas, liver, and kidney (Table S1). These results indicate that Stab2 is dispensable for normal development and viability in mice.

Given that Stab2 is a known scavenger receptor that binds and eliminates from the circulation various substances, including HA, ac-LDL, and heparin (4, 27, 28), we assessed the circulating levels of these substances in Stab2 KO mice. Although serum levels of ac-LDL and heparin were unchanged in the Stab2 KO mice (Table S1), serum HA levels were dramatically increased, by as much as 59-fold over control values (Fig. 1*A*). Because HA's molecular size affects its function (16), we next analyzed the molecular size of serum HA by electrophoresis using Stains-All (which stains negatively charged molecules), and estimated it as ~40 kDa (Fig. S1*J*). Given that >90% of the circulating HA is cleared by HSECs (1), and that Stab2 is specifically expressed in HSECs, we examined whether the high serum HA levels in Stab2 KO mice were due to impaired endocytosis. We prepared HSECs from WT and Stab2 KO mice and quantitatively evaluated their endocytotic activity based on the internalization of FITC-labeled HA and DiI-labeled ac-LDL (DiI-Ac-LDL) (Fig. 1*B* and *C* and Fig. S1 *K* and *L*). Although there was no significant difference in the internalization of DiI-Ac-LDL between WT and Stab2 KO mice, the internalization of HA into Stab2-deficient HSECs was markedly decreased, to only ~8% of the WT level. We also examined the expression of other HA receptors (CD44 and Lyve-1) and HA synthases (HAS1, HAS2, and HAS3) that can potentially affect HA levels, but found no significant changes in the Stab2 KO mice (Fig. S2 *A* and *B*). These results provide clear evidence that Stab2 is the major clearance receptor for HA in the body.

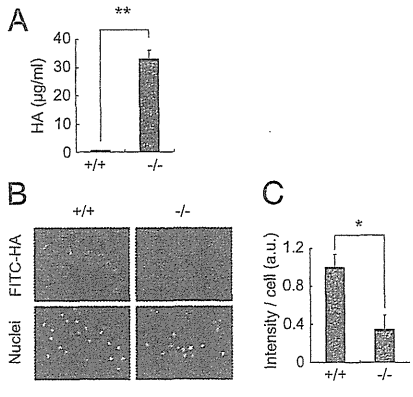

Fig. 1. Serum HA levels and internalization of HA in Stab2-deficient cells. (*A*) Serum HA levels in WT ($^{+/+}$) and homozygous ($^{-/-}$) littermates ($n = 3$; $^{**}P < 0.01$). (*B*) Internalization of FITC-HA in Percoll-purified HSECs from Stab2$^{+/+}$ and Stab2$^{-/-}$ littermates. (*Upper*) Fluorescence of FITC-HA incorporated into cells. (*Lower*) Hoechst 33342 staining. (*C*) Quantification of FITC fluorescence intensity ($n = 4$; $^{*}P < 0.05$).

Metastasis of Melanoma Cells Is Suppressed in Stab2 KO Mice. The elevation in serum HA levels in Stab2 KO mice prompted us to examine whether the lack of Stab2 has any effects on tumorigenesis. B16 melanoma cells are known to form tumor nodules in the lung when injected i.v. We administered B16F10 cells i.v. in littermates of Stab2$^{+/+}$ and Stab2$^{-/-}$ mice. After 14 d, numerous black nodules had formed on the lung surfaces of the Stab2$^{+/+}$ mice, but surprisingly, nodular formation was markedly reduced in Stab2$^{-/-}$ mice (Fig. 2 *A* and *B*). In contrast, tumor formation resulting from the s.c. inoculation of melanoma cells did not differ significantly between the Stab2$^{+/+}$ and Stab2$^{-/-}$ mice (Fig. 2*C*). Moreover, our in vitro experiments showed that the proliferation of B16F10 cells was not affected by HA, and a cell cycle analysis of B16F10 cells recovered from lung tumors revealed no difference between the Stab2 KO and WT mice (Fig. S3*A*). These results indicate that the metastasis, but not the proliferation, of melanoma cells was affected by the lack of Stab2.

To analyze the early stages of metastasis, we also conducted imaging in vivo, because the nodules of B16F10 cells at day 7 were too small to count. B16F10 cells were stably transfected with the firefly luciferase gene to generate B16F10-luc-G5 cells,

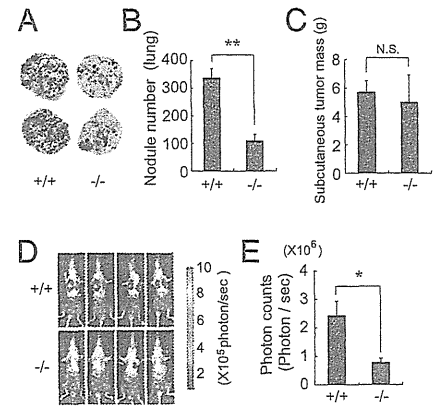

Fig. 2. Homing of B16F10 melanoma to the lungs in Stab2 KO mice. B16F10 cells (5×10^5) were injected via the tail vein in Stab2$^{+/+}$ and Stab2$^{-/-}$ littermates. (*A*) Metastatic nodules formed on the lungs at day 14 after the injection. (*B*) Numbers of nodules formed on the lungs were counted manually ($^{+/+}$, $n = 9$; $^{-/-}$, $n = 6$; $^{**}P < 0.01$). (*C*) Size of tumors formed by s.c. inoculated melanoma cells at day 21 [$^{+/+}$, $n = 8$; $^{-/-}$, $n = 6$; $^{*}P > 0.05$ (not significant)]. (*D*) Metastasis of i.v. injected B16F10-luc-G5 cells measured by luminescence using IVIS in vivo imaging at day 7. (*E*) Quantification of photon counts in *C* ($^{+/+}$, $n = 6$; $^{-/-}$, $n = 5$; $^{*}P < 0.05$).

which were then injected i.v. into littermates of Stab2$^{+/+}$ and Stab2$^{-/-}$ mice. After 7 d, tumor metastasis was measured based on the luminescence of luciferase. Photon counts were significantly decreased in the Stab2$^{-/-}$ mice, indicating inhibition of metastasis at an early stage (Fig. 2 *D* and *E*).

Administration of Anti-Stab2 Antibody Increases Serum HA Levels and Prevents Tumor Metastasis. We next investigated whether Stab2 functions could be blocked by an anti-Stab2 antibody in vivo. We generated several mAbs against the extracellular domain of Stab2 by immunizing rats with BaF3 cells expressing Stab2 and one of them (#34-2, ref. 10) was found to inhibit HA binding to Stab2 as assessing by internalization of FITC-labeled HSECs in vitro (Fig. 3*A*). To test whether that anti-Stab2 mAb has any effect on the plasma HA level in vivo, we injected it i.p. into C57BL/6 mice every 3 d and monitored serum HA levels. Within 3 d of the first injection, serum HA levels were increased in all of the mice given the anti-Stab2 mAb, but not in the mice treated with rat IgG (Fig. 3*B*). We obtained the same results using SCID mice (Fig. 4 *A* and *J*). These findings clearly indicate that the anti-Stab2 mAb effectively increased plasma HA levels by inhibiting Stab2 function in vivo. To examine whether this mAb prevents tumor metastasis, we injected mice with either anti-Stab2 mAb or control rat IgG, followed 2 d later by i.v. injection of B16F10 cells. The anti-Stab2 mAb significantly suppressed metastasis (Fig. 3 *C* and *D*). Taken together, these results indicate that the anti-Stab2 mAb elevates circulating HA levels by blocking the clearance of HA in HSECs, and that serum HA levels are inversely correlated with tumor metastasis.

Because the anti-Stab2 mAb elevated plasma HA levels in immune deficient mice, we investigated its effect on spontaneous metastasis by multiple cancer cells in SCID mice. To do so, we transplanted MDA-MB-231-luc-D3H2LN cells (human mammary gland adenocarcinoma cells expressing luciferase) into the abdominal mammary glands of SCID mice. After 21 d, tumor metastasis in the upper body, including the brachial lymph nodes, was evaluated by luminescence analysis. The number of photons derived from metastasized cells in the upper body was significantly reduced in the mice treated with the anti-Stab2 mAb (Fig. 4 *A–D*). We also transplanted 4T1-LucNeo-1H mouse mammary tumor cells expressing luciferase into the mammary fad pads of the mice. Starting at 2 d after tumor injection, each animal was given either anti-Stab2 mAb or rat IgG every 3 d. At 3 wk after the start of antibody treatment, metastatic luminescence signals and the numbers of histological lesions in the lung were reduced in the anti-Stab2 mAb-treated mice. Given the lack of significant difference in the size of primary tumors (Fig. 4 *E–L*), anti-Stab2 mAb can be considered to inhibit spontaneous metastasis.

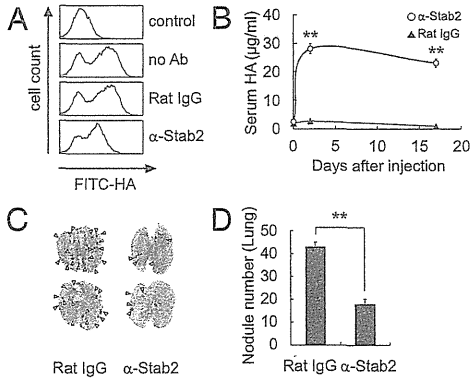

Fig. 3. Inhibition of HA clearance and metastasis by anti-Stab2 mAb. (*A*) HSECs were incubated with anti-Stab2 mAb or rat IgG, and the cell internalization of FITC-HA was analyzed by flow cytometry. (*B*) Anti-Stab2 mAb or rat IgG (3 mg/kg body weight) was administered i.p. to C57BL/6 mice on days 0, 3, and 17, and serum HA levels were measured ($n = 5$; $^{**}P < 0.01$). (*C*) At 2 d after the i.p. administration of anti-Stab2 mAb or control IgG, 5×10^4 B16F10 cells were injected i.v. via the tail vein. Anti-Stab2 mAb or control IgG was administered every 3 d. The lungs at 14 d are shown. Arrowheads indicate nodules of B16F10 cells. (*D*) The number of nodules formed on the lungs were counted manually ($n = 10$; $^{**}P < 0.01$). α-Stab2 denotes anti-Stab2 mAb.

Examination of Possible Mechanisms for Inhibition of Metastasis. To investigate the inhibitory mechanism of metastasis observed in the Stab2 KO and anti-Stab2 mAb-treated mice, we first analyzed whether HA affects tumor cells in vitro. We evaluated the effects of a 31-kDa HA (similar in size to HA in circulation; Fig. S1*J*), on cell proliferation, apoptosis induced by hydrogen peroxide, migration, and invasion into the basal membrane. None of these assays demonstrated any significant effect of HA on tumor cells at various concentrations (Fig. S3 *A–E*).

Because the proliferation as well as metastasis of tumors is under surveillance by the immune system, and HA has been implicated in the immune system, we examined the immune cells of Stab2 KO mice for any changes. We found no significant differences in fractions of regulatory T cells, NK cells, macrophages, and myeloid-derived suppressor cells in bone marrow, peripheral blood, and spleen in Stab2 KO mice compared with WT mice (Fig. S4*A*). In addition, we found no alterations in serum levels of TNF-α, IFN-γ, IL-2, IL-4, IL-6 IL-10, and IL-17A (Fig. S4*B*), or in the activation of macrophages in vivo and sensitivity to i.p. LPS (Figs. S2*E* and S4*C*). These results showing no significant alterations in the immune system in Stab2 KO mice suggest that the immune system may not be directly involved in the inhibition of tumor metastasis.

Attachment of Melanoma Cells to the Lungs Is Prevented by an Increase in Plasma HA. Intravenously injected melanoma cells are thought to roll through the bloodstream and lodge in the lungs, where they proliferate. Our finding that the melanoma cells injected s.c. in Stab2 KO mice formed tumors as large as those seen in their WT littermates (Fig. 2*C*) suggests that the homing of i.v. injected tumor cells to the lungs might be altered in the mutant mice. To analyze the attachment of melanoma cells to the lung in vivo, we inoculated B16F10-luc-G5 cells i.v. After 6 h, mice were perfused with PBS via the portal vein to remove blood cells from the tissues, and luciferase activity in the lungs was evaluated. The luciferase activity in the lungs was significantly decreased in Stab2 KO mice and in mice treated with the anti-Stab2 mAb compared with WT mice and rat IgG-treated mice (Fig. 5 *A* and *B*). These results indicate that tumor metastasis was prevented at an early stage of penetration in the lungs.

Because plasma HA level has been suggested to be involved in the metastasis of melanoma cells, and HA binds to cell surface molecules such as CD44, we investigated whether HA mediates the attachment of tumor cells to tissues. We first tested the binding of melanoma cells to HA by plating B16F10 cells on an HA-coated plate, and found that the cells attached to the plate via HA (Fig. S3*F*). Adding HA at the concentration found in Stab2 KO mouse sera inhibited the binding of B16F10 to the HA-coated plate. This finding suggests that the increased plasma HA in the mutant mice inhibits metastasis by preventing the attachment of melanoma cells to the lung via HA.

We also investigated whether HA prevents the attachment of B16F10 cells to the lung. Although i.v. injected HA is rapidly cleared from the bloodstream (1), we found that a very high dose of HA administered via the tail vain elevated the serum HA level for several hours (Fig. 5*C*). Thus, we injected HA at a dose of 20 mg/kg body weight every 8 h for 24 h to increase the plasma HA level, and then transplanted B16F10-luc-G5 cells. At 6 h after B16F10-luc-G5 cell transplantation, luciferase activity in the lungs was significantly reduced, whereas the serum

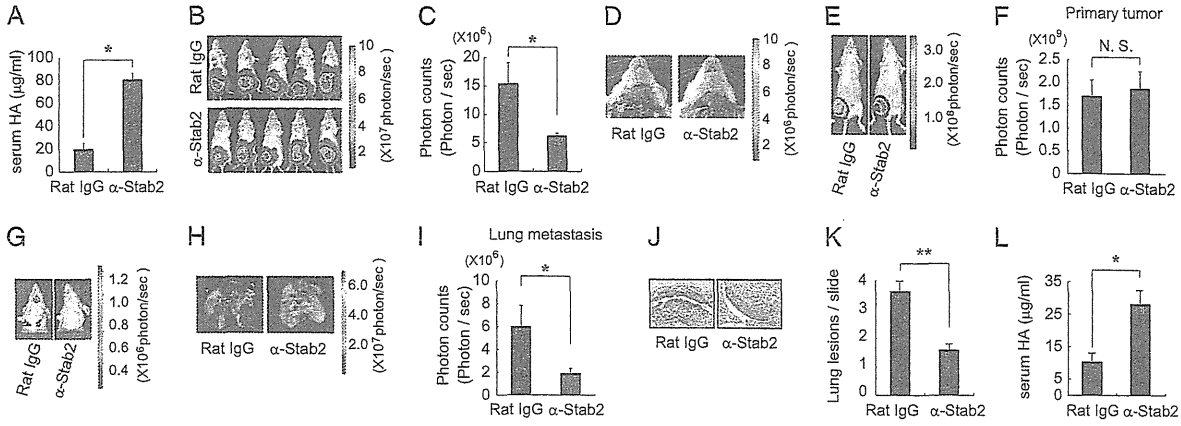

Fig. 4. Anti-Stab2 antibody prevents spontaneous metastasis of human and mouse mammary tumor cells in SCID mice. (*A*) SCID mice were i.p. injected with anti-Stab2 mAb or rat IgG (3 mg/kg), and serum HA levels were measured at 7 d after the injection ($n = 5$; $^*P < 0.05$). (*B*) MDA-MB-231-luc-D3H2LN cells were grafted in the mammary gland of SCID mice injected i.p. with anti-Stab2 mAb or control IgG (3 mg/kg). Luminescence was measured by IVIS at day 21. (*C*) Quantification of photon counts in the upper body at day 21 ($n = 5$; $^*P < 0.05$). (*D*) Luminescence of the opened thorax in *B*. (*E*) Mouse 4T1-LucNeo-1H mammary tumor cells were grafted into a mammary fat pad of the mice. At 2 d after tumor injection, each animal was given anti-Stab2 mAb or Rat IgG i.p. every 3 d, for a total of seven injections. Luminescence of primary tumors was measured by IVIS at day 21. (*G*) For the detection of signals from metastatic regions, the lower part of each animal was shielded with black paper before reimaging, to minimize bioliminescence from primary tumor. At the end of the experiment (day 21), ex vivo imaging was performed on collected lungs. Control group mice exhibited spontaneous lung metastasis. (*F*, *H*, and *I*) Quantification of bioluminescence emitted from primary tumors on mice and lung metastatic regions at the end of the experiment. Data represent mean ± SD ($n = 4$; $^*P < 0.05$ vs. other groups). (*J*) H&E-stained sections of spontaneous lung metastasis lesions at day 21. (*K*) Quantification of lung lesions in *J*. Data represent mean values ($n = 32$; $^{**}P < 0.01$ vs. other groups). (*L*) Serum HA levels measured at the end of the experiment ($n = 4$; $^*P < 0.05$). α-Stab2 denotes anti-Stab2 mAb.

HA level remained elevated in those mice pretreated with HA (Fig. 5 *D* and *E*).

Finally, to prove that increased HA level decreases the arrest of tumor cells in lung capillaries, we performed in vitro rolling/tethering assays using a VenaEC system. Pulmonary ECs from WT mice were cultured on VenaEC substrates and connected to a microfluidic device. Rolling/tethering between pulmonary cells and B16 melanoma cells under share stress was observed (Fig. 5*F*). At a low HA concentration (0.55 μg/mL, similar to Stab2$^{+/+}$ serum levels), B16 melanoma cells were tethered to pulmonary

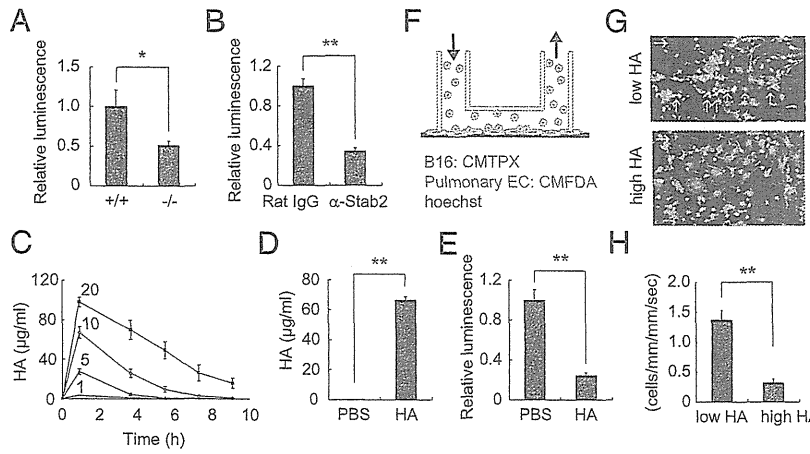

Fig. 5. HA inhibits attachment of B16F10 cells. (*A*) B16F10-luc-G5 cells (1.5×10^6) were injected into the tail vein of Stab2$^{+/+}$ and Stab2$^{-/-}$ mice, and 6 h later, the mice were perfused with PBS via the portal vein to remove blood cells from tissues. The B16F10-luc-G5 cells remaining in the lungs were detected by luciferase analysis ($^{+/+}$, $n = 6$; $^{-/-}$, $n = 7$; $^*P < 0.05$). (*B*) At 2 d after the i.p. administration of anti-Stab2 or rat IgG, B16F10-luc-G5 cells (1.5×10^6) were injected into the tail vein. At 6 h later, the injection cells remaining in the lungs were detected by luciferase analysis as in *A* (rat IgG, $n = 5$; $^{-/-}$, $n = 6$; $^{**}P < 0.01$). (*C*) HA at doses of 1, 5, 10, and 20 mg/kg was injected i.v., and serum HA levels were measured serially ($n = 4$). (*D*) HA at 20 mg/kg or an equal volume of PBS was injected i.v. every 8 h. At 24 h after the first HA injection, B16F10-luc-G5 cells (1.5×10^6) were injected into the tail vein with 20 mg/kg of HA. After 6 h, serum samples were collected, and plasma HA levels were analyzed at the end of experiment ($n = 8$; $^{**}P < 0.01$). (*E*) Cells remaining in the lungs were detected based on luciferase activity at *D* as in *A* ($n = 8$; $^{**}P < 0.01$). (*F*) Schematic diagram of the VenaEC system (Cellix). (*G*) Rolling and/or tethering of B16 melanoma cells onto pulmonary ECs using the VenaEC system. Pulmonary ECs from 6-d-old WT (C57BL/6) mice were isolated, cultured, and stained with 5 μM CMFDA (green) and 10 μM Hoechst 33342 (blue). B16F10 cells were stained with 5 μM CMTPX (red) and 10 μM Hoechst (blue). The pulmonary cell chamber was connected to a microfluidic device, and perfusion for 5 min with VL medium containing stained B16F10 cells at 0.7 dynes/cm^2 was performed during confocal observation of cell kinetics. Representative images of B16 melanoma cells with low (0.55 μg/mL) and high (33 μg/mL) HA concentrations are shown (Movies S1 and S2). White arrows denote flow directions, and red arrows indicate rolling and/or tethering B16F10 cells. (*H*) Quantification of rolling/tethering to the pulmonary ECs. The numbers of rolling/ tethering B16F10 cells were counted. Note that HA at high concentrations inhibited the rolling/tethering of melanoma cells onto pulmonary endothelium ($n = 20$ images from five experiments; $^*P < 0.05$). (Scale bar: 100 μm.) α-Stab2 denotes anti-Stab2 mAb.

cells. In contrast, at a high HA concentration (33 μg/mL, similar to Stab2$^{-/-}$ serum levels), tethering was significantly reduced (Fig. 5 *G* and *H* and Movies S1 and S2). These results indicate that a high level of HA in the circulation prevents the attachment of melanoma cells to the lung.

Discussion

In this study, using Stab2 KO mice and an anti-Stab2 mAb, we provide several lines of evidence indicating that Stab2 is the major clearance receptor for circulating HA. This finding is consistent with the results of a previous in vitro study showing that Stab2, not its homolog Stab1, is the major clearance receptor for HA (5), as well as a recent study using Stab1 and Stab2 KO mice (2). In addition, KO mice deficient in either Lyve1 or Stab1 showed no change in serum HA levels (2, 29), further supporting this idea. Although Stab2 is known to bind other molecules, such as ac-LDL and heparin, serum levels of ac-LDL and heparin were not increased in the Stab2 KO mice, and the internalization of ac-LDL into Stab2-deficient HSECs was normal, indicating that those molecules are cleared by other scavenger receptors, such as Stab1. Therefore, we conclude that Stab2 is the bona fide clearance receptor for circulating HA in vivo.

An unexpected finding—and perhaps the most important result of this study—is the markedly reduced metastasis of melanoma cells in the Stab2 KO mice. Furthermore, i.p. administration of the blocking mAb for Stab2 also increased the serum concentration of HA and inhibited tumor metastasis in the Stab2$^{+/+}$ mice at levels comparable to those in Stab2 KO mice (Fig. 3). The KO mice were fertile, developed normally, and exhibited no hematological or histological changes except for the increased serum HA level (Fig. S1 and Table S1). Although Stab2 has multiple ligands, only HA levels were altered in the Stab2 KO mice, and the anti-Stab2 mAb caused phenotypes similar to those in the Stab2 KO mice. Thus, we focused on HA to investigate the mechanism preventing metastasis, and carried out various experiments in vitro and in vivo. Our in vitro experiments indicated that HA did not affect the proliferation, migration, and invasion of B16F10 cells (Fig. S3 *A–E*). Moreover, the weights of tumors formed by s.c. transplanted melanoma cells, as well as the cell cycle status of i.v. injected melanoma cells, were not changed in the Stab2 KO mice, indicating that the lack of Stab2 does not affect tumor proliferation in vivo (Fig. 2*C* and Fig. S3*B*). Likewise, mammary tumor cells formed primary tumors in abdominal fat pads, but tumor formation in the lymph nodes or lung was severely suppressed by anti-Stab2 mAb (Fig. 4). These results strongly suggest that tumor metastasis is prevented by a mechanism other than proliferation.

Tumorigenesis is controlled by the immune system, and the role of HA in the immune system has been studied extensively. Of note, HA binds to TLR2 and TLR4, which play important roles in innate immunity (18). We examined several parameters of the immune system, focusing first on macrophage functions, given that HA has been shown to alter immune responses via TLR4 that binds to LPS (18). However, macrophage activation and the severity of sepsis induced by i.p. injected LPS were not changed in Stab2 KO mice or in mice treated with the anti-Stab2 mAb (Figs. S2*E* and S4*C*). Furthermore, levels of inflammatory cytokines in serum and populations of various immune cells were not affected (Fig. S4 *A* and *B*). Therefore, inhibition of Stab2 function does not appear to directly affect the immune system. It is known that HA's functions depend on its molecular size, which varies from a few kDa to a few MDa (16). In the present study, HA molecules in Stab2 KO serum were ~40 kDa in size (Fig. S1*J*). possibly explaining some of the discrepancy between our results and those of previous studies.

Tumor cells circulate through the bloodstream and penetrate preferable tissues. Given that the s.c. proliferation of melanoma cells in Stab2 KO mice was not altered (Fig. 2*C*), we examined the initial step of attachment to the lungs. Melanoma cells expressing luciferase were injected via the tail vein, and cells trapped in the lungs were detected based on luciferase activity after perfusion with PBS to remove nonadherent cells. At 6 h after the i.v. injection, the number of melanoma cells trapped in the lungs was decreased in both the Stab2 KO mice and the mice given anti-Stab2, indicating that tumor metastasis is prevented at the initial stage of tissue penetration in the absence of Stab2 function (Fig. 5 *A* and *B*). Because those mice had extremely high plasma HA levels, we considered that the attachment of melanoma cells to the lungs is enhanced by HA displayed on the surface of blood vessels in normal lungs, and that a high level of HA in plasma blocks this interaction. In fact, melanoma cells adhered to HA-coated plates and pulmonary ECs, and HA at high concentrations, similar to those in serum of Stab2 KO mice, inhibited the attachment (Fig. 5, Fig. S3*F*, and Movies S1 and S2). Although i.v. injected HA is rapidly removed from the circulation, we found that the i.v. injection of a very high dose of HA was able to maintain the plasma HA concentration at a high level for at least 10 h (Fig. 5*C*). After the circulating HA level increased, B16F10 cells were injected to evaluate their attachment to the lungs. Metastasis of B16F10 cells to the lungs was markedly suppressed under these conditions (Fig. 3*D*). These results strongly suggest that inhibition of Stab2 function prevents tumor metastasis by elevating the plasma HA level.

Previous studies found that forced expression of HAS increased tumor cell proliferation and metastasis, whereas inhibition of HAS prevented proliferation and metastasis (23, 24, 30). These experiments suggested that HA promotes tumor proliferation and metastasis, whereas our results indicate that HA prevents metastasis. The critical difference between the previous studies and the present study is that we focused on the circulating HA, whereas most of the previous studies investigated extracellular matrix and pericellular HA. Therefore, it seems that the function of HA can differ depending on location.

In conclusion, our Stab2 KO mice were viable and exhibited no overt defects, but had dramatically increased plasma HA levels. This indicates that Stab2 is dispensable for normal development and homeostasis, and that an extremely high level of plasma HA has no deleterious effect. The increase in circulating HA levels was inversely correlated with metastasis and inhibited the attachment of melanoma cells to the lungs. Moreover, the administration of an anti-Stab2 mAb also increased the plasma HA level and blocked the metastasis of not only mouse melanoma cells, but also human breast tumor cells with no side effects. Thus, functional inhibition of Stab2 may be a potential strategy to suppress tumor metastasis.

Materials and Methods

A Stab2 KO mouse line was generated by conventional methods, as described in *SI Materials and Methods*, and backcrossed with C57BL/6 for at least six generations. Anti-mouse Stab2 mAb (#34-2) was generated in our laboratory (10). Serum HA levels were measured with an HA assay kit (Seikagaku Biobusiness) in accordance with the manufacturer's instructions. The cell internalization of FITC-HA into HSECs was performed as described previously (10). For FACS analysis, HSECs were incubated with indicated antibodies and FITC-HA, and labeled cells were analyzed with a FACSCalibur flow cytometer (BD Biosciences). B16F10 cells [5×10^5 (Fig. 2) or 5×10^4 (Fig. 3)] were injected into the tail vein. At 14 d after injection, the lung surface nodules were counted. For imaging in vivo, 5×10^5 B16F10-luc-G5 cells were injected i.v. At 7 d after the injection, metastasis was analyzed with luciferase luminescence as described previously (31). MDA-MB-231-luc-D3H2LN cells (4×10^6) were injected into the mammary gland of SCID mice, and metastasis was analyzed using the IVIS imaging system (31, 32). 4T1-LucNeo-1H cells (5×10^4) were injected into a mammary fad pad of SCID mice. Rolling and/or tethering of B16 melanoma cells onto cultured pulmonary ECs was analyzed under flow conditions at 0.7 dynes/cm^2 with the VenaEC System (Cellix) using confocal microscopy (Nikon A1R). Before the experiments, B16 melanoma cells were stained by CellTracker Red CMTPX (Molecular Probes) and Hoechst 33342 (Molecular Probes). Pulmonary ECs were also stained with CellTracker Green CMFDA (Molecular Probes) and Hoechst 33342. More detailed information is provided in *SI Materials and Methods*.

ACKNOWLEDGMENTS. We thank Dr. T. Akiyama for providing the B16F10 cells and Drs. H. Saya, T. Itoh, and M. Tanaka for valuable discussions and a critical reading of the manuscript. We also thank M. Tajima, C. Yoshinaga, and X. Yingda for their excellent technical help. This work was supported in part by research grants from the Ministry of Education, Culture, Sports, Science and Technology (MEXT) of Japan and the Ministry of Health, Labor and Welfare (MHLW) of Japan (to A.M.); the Centers of Research Excellence in Science and Technology program (A.M); the A-STEP program of the Japan Science and Technology Agency (Y.H.) and Takeda Science Foundation (to A.M.); the Funding Program for Next Generation World-Leading Researchers (to S.N.); the Japan Society for the Promotion of Science through its Funding Program for World-Leading Innovative Research and Development on Science and Technology (FIRST Program) (R.N.); Research Fellowships from a Grant-in-Aid 22113008 for Scientific Research on Innovative Areas of Fluorescence Live Imaging from The Ministry of Education, Culture, Sports, Science, and Technology of Japan (to S.N.); Grants-in-Aid for Scientific Research (to R.N.), grants for Translational Systems Biology and Medicine Initiative (to S.N. and R.N.), and the global Centers of Excellence program from the MEXT of Japan (R.N.); Banyu Life Science Foundation International (S.N.); and a research grant from the National Institute of Biomedical Innovation (to R.N.).

1. Fraser JR, Alcorn D, Laurent TC, Robinson AD, Ryan GB (1985) Uptake of circulating hyaluronic acid by the rat liver: Cellular localization in situ. *Cell Tissue Res* 242: 505–510.
2. Schledzewski K, et al. (2011) Deficiency of liver sinusoidal scavenger receptors stabilin-1 and -2 in mice causes glomerulofibrotic nephropathy via impaired hepatic clearance of noxious blood factors. *J Clin Invest* 121:703–714.
3. Politz O, et al. (2002) Stabilin-1 and -2 constitute a novel family of fasciclin-like hyaluronan receptor homologues. *Biochem J* 362:155–164.
4. Adachi H, Tsujimoto M (2002) FEEL-1, a novel scavenger receptor with in vitro bacteria-binding and angiogenesis-modulating activities. *J Biol Chem* 277:34264–34270.
5. Hansen B, et al. (2005) Stabilin-1 and stabilin-2 are both directed into the early endocytic pathway in hepatic sinusoidal endothelium via interactions with clathrin/AP-2, independent of ligand binding. *Exp Cell Res* 303:160–173.
6. Kzhyshkowska J, et al. (2005) Phosphatidylinositide 3-kinase activity is required for stabilin-1–mediated endosomal transport of acLDL. *Immunobiology* 210:161–173.
7. Kzhyshkowska J, et al. (2008) Alternatively activated macrophages regulate extracellular levels of the hormone placental lactogen via receptor-mediated uptake and transcytosis. *J Immunol* 180:3028–3037.
8. Kzhyshkowska J, et al. (2006) Novel function of alternatively activated macrophages: Stabilin-1-mediated clearance of SPARC. *J Immunol* 176:5825–5832.
9. Salmi M, Koskinen K, Henttinen T, Elima K, Jalkanen S (2004) CLEVER-1 mediates lymphocyte transmigration through vascular and lymphatic endothelium. *Blood* 104: 3849–3857.
10. Nonaka H, Tanaka M, Suzuki K, Miyajima A (2007) Development of murine hepatic sinusoidal endothelial cells characterized by the expression of hyaluronan receptors. *Dev Dyn* 236:2258–2267.
11. Park SY, et al. (2008) Rapid cell corpse clearance by stabilin-2, a membrane phosphatidylserine receptor. *Cell Death Differ* 15:192–201.
12. Gustafson S, Björkman T (1997) Circulating hyaluronan, chondroitin sulphate and dextran sulphate bind to a liver receptor that does not recognize heparin. *Glycoconj J* 14:561–568.
13. Harris EN, Weigel PH (2008) The ligand-binding profile of HARE: Hyaluronan and chondroitin sulfates A, C, and D bind to overlapping sites distinct from the sites for heparin, acetylated low-density lipoprotein, dermatan sulfate and CS-E. *Glycobiology* 18:638–648.
14. Kogan G, Soltés L, Stern R, Gemeiner P (2007) Hyaluronic acid: A natural biopolymer with a broad range of biomedical and industrial applications. *Biotechnol Lett* 29: 17–25.
15. Fraser JR, Laurent TC, Laurent UB (1997) Hyaluronan: Its nature, distribution, functions and turnover. *J Intern Med* 242:27–33.
16. Stern R, Asari AA, Sugahara KN (2006) Hyaluronan fragments: An information-rich system. *Eur J Cell Biol* 85:699–715.
17. Almond A (2007) Hyaluronan. *Cell Mol Life Sci* 64:1591–1596.
18. Jiang D, et al. (2005) Regulation of lung injury and repair by Toll-like receptors and hyaluronan. *Nat Med* 11:1173–1179.
19. DeGrendele HC, Estess P, Siegelman MH (1997) Requirement for CD44 in activated T cell extravasation into an inflammatory site. *Science* 278:672–675.
20. Zöller M (2011) CD44: Can a cancer-initiating cell profit from an abundantly expressed molecule? *Nat Rev Cancer* 11:254–267.
21. Banerji S, et al. (1999) LYVE-1, a new homologue of the CD44 glycoprotein, is a lymph-specific receptor for hyaluronan. *J Cell Biol* 144:789–801.
22. Kim S, et al. (2009) Carcinoma-produced factors activate myeloid cells through TLR2 to stimulate metastasis. *Nature* 457:102–106.
23. Sironen RK, et al. (2011) Hyaluronan in human malignancies. *Exp Cell Res* 317: 383–391.
24. Toole BP (2004) Hyaluronan: From extracellular glue to pericellular cue. *Nat Rev Cancer* 4:528–539.
25. Twarock S, et al. (2011) Inhibition of oesophageal squamous cell carcinoma progression by in vivo targeting of hyaluronan synthesis. *Mol Cancer* 10:30.
26. Kudo D, et al. (2004) Effect of a hyaluronan synthase suppressor, 4-methylumbelliferone, on B16F-10 melanoma cell adhesion and locomotion. *Biochem Biophys Res Commun* 321:783–787.
27. Zhou B, Weigel JA, Fauss L, Weigel PH (2000) Identification of the hyaluronan receptor for endocytosis (HARE). *J Biol Chem* 275:37733–37741.
28. Harris EN, Weigel JA, Weigel PH (2008) The human hyaluronan receptor for endocytosis (HARE/Stab2) is a systemic clearance receptor for heparin. *J Biol Chem* 283: 21453–21461.
29. Gale NW, et al. (2007) Normal lymphatic development and function in mice deficient for the lymphatic hyaluronan receptor LYVE-1. *Mol Cell Biol* 27:595–604.
30. Yoshihara S, et al. (2005) A hyaluronan synthase suppressor, 4-methylumbelliferone, inhibits liver metastasis of melanoma cells. *FEBS Lett* 579:2722–2726.
31. Takeshita F, et al. (2005) Efficient delivery of small interfering RNA to bone-metastatic tumors by using atelocollagen in vivo. *Proc Natl Acad Sci USA* 102:12177–12182.
32. Jenkins DE, Hornig YS, Oei Y, Dusich J, Purchio T (2005) Bioluminescent human breast cancer cell lines that permit rapid and sensitive in vivo detection of mammary tumors and multiple metastases in immune deficient mice. *Breast Cancer Res* 7:R444–R454.

frontiers in GENETICS

REVIEW ARTICLE
published: 03 January 2012
doi: 10.3389/fgene.2011.00097

Unraveling the mystery of cancer by secretory microRNA: horizontal microRNA transfer between living cells

Nobuyoshi Kosaka and Takahiro Ochiya*

Division of Molecular and Cellular Medicine, National Cancer Center Research Institute, Tokyo, Japan

Edited by:
Michael Rossbach, Genome Institute of Singapore, Singapore

Reviewed by:
Lauren Averett Byers, UT MD Anderson Cancer Center, USA
Leonard Lipovich, Wayne State University, USA
Raffaele A. Calogero, University of Torino, Italy

***Correspondence:**
Takahiro Ochiya, Division of Molecular and Cellular Medicine, National Cancer Center Research Institute, 5-1-1, Tsukiji, Chuo-ku, Tokyo 104-0045, Japan.
e-mail: tochiya@ncc.go.jp

microRNAs (miRNAs) have been identified as a fine-tuner in a wide array of biological processes, including development, organogenesis, metabolism, and homeostasis. Deregulation of miRNAs causes diseases, especially cancer. This occurs through a variety of mechanisms, such as genetic alterations, epigenetic regulation, or altered expression of transcription factors, which target miRNAs. Recently, it was discovered that extracellular miRNAs circulate in the blood of both healthy and diseased patients. Since RNase is abundant in the bloodstream, most of the secretory miRNAs are contained in apoptotic bodies, microvesicles, and exosomes or bound to the RNA-binding proteins. However, the secretory mechanism and biological function, as well as the significance of extracellular miRNAs, remain largely unclear. In this article, we summarize the latest and most significant discoveries in recent peer-reviewed research on secretory miRNA involvement in many aspects of physiological and pathological conditions, with a special focus on cancer. In addition, we discuss a new aspect of cancer research that is revealed by the emergence of "secretory miRNA."

Keywords: secretory microRNA, microRNA, exosome, cell–cell communication, cancer

INTRODUCTION

microRNAs (miRNAs) are small non-coding RNA that repress a wide variety of target genes expression at the post-transcriptional level by sequence-specific base pairing to the 3′ untranslated region of multiple target mRNAs. They are conserved through species, and form an important class of regulators that participate in multiple biological phenomena, including development, organogenesis, and homeostasis. Because of their ability to bind to many target mRNAs (Kwak et al., 2011), once their expression is altered, disease could occur through the deregulation of their target gene networks, particularly that leading to cancer. For this reason, many recent studies have focused on the development of novel diagnosis and therapeutics in the field of oncology. Current studies have revealed that miRNAs are secreted outside of the cells, and their biological significance is beginning to be recognized (Zernecke et al., 2009; Kosaka et al., 2010b; Pegtel et al., 2010). This article is a summary of the latest and most significant findings of original studies on the involvement of secretory miRNAs in cancer, with a special focus on the potential of secretory miRNAs as a humoral factor for cancer biology.

RNA IS NOT ONLY THE MEDIATOR IN THE CENTRAL DOGMA BUT ALSO A SECRETORY FUNCTIONAL MOLECULE

Before Watson and Crick (1953) described the double-helical structure of the DNA molecule, Mandel and Metais (1947) had found that DNA is present in plasma and serum in 1947. They showed the presence of nucleic acids in healthy subjects as well as in ill patients. After that, many researchers have tried to examine the circulating nucleic acid to develop them as a potential biomarker, especially in the research field of cancer (Fleischhacker and Schmidt, 2007). It is now well documented that RNA can also be detected in plasma, serum, and other body fluids as well as from cell-free supernatants of *in vitro* cultivated cells. One of the first papers demonstrating the presence of extracellular RNA was published by Stroun et al. (1978). They reported the presence of an RNA form in a nucleoprotein complex spontaneously released from human blood lymphocytes and frog cell systems from auricle cultures. They also showed that the RNA from this complex has a stimulating effect on DNA synthesis *in vitro*, suggesting the function of secretory RNA in recipient cells.

Meanwhile, the uptake of RNA by recipient cells was also observed. More than 40 years ago, RNAs were reported to be readily taken up by ascites tumor cells (Galand and Ledoux, 1966). In addition, during a study of co-cultured cells that were previously incubated with or without tantalum particles, intact labeled RNA was found to be transferred into the non-labeled recipient cells from labeled donor cells (Kolodny, 1971). Namely, cell–cell communication was mediated not only by proteins, such as cytokines, chemokines, and hormones, but also by secretory RNA.

Given that the concentration of RNA-degrading enzymes, RNase, is high in normal people and even higher in cancer patients (Reddi and Holland, 1976; Tsui et al., 2002) and that RNase is extremely stable, it was reasoned that the RNA released from the cells into the extracellular space must be complexed and in a form that is resistant against RNases. The first study of associating circulating RNA, as RNA–proteolipid complexes, in serum was reported in 1987 (Wieczorek et al., 1987). This study reported a relationship between the presence of RNA–proteolipid complexes and tumor mass/response to therapy. These complexes disappeared ~48 h after tumor removal and were undetected in benign disorders. Another study demonstrated that the release of a macromolecular substance containing ^{32}P and ^{3}H was found when prelabeled

Chinese hamster ovary cells were treated with trypsin under conditions in which cells remain fully viable (Rieber and Bacalao, 1974). In contrast, a ribonuclease treatment affected neither the ^{32}P nor the ^{3}H radioactivity. The authors concluded from these experiments that RNA together with glycoproteins is released from the external cell surface.

FUNCTIONAL IMPORTANCE OF SECRETORY miRNA IN VARIOUS KINDS OF LIFE PHENOMENA

miRNAs, a class of post-transcriptional gene expression regulators, play critical roles in various kinds of biological phenomena, including development, organogenesis, and homeostasis. Dysregulation of miRNA leads to cancer development and progression and has different expression profiles in normal tissues and cancers (Garzon et al., 2010). For this reason, miRNAs have been investigated for their potential use in the diagnosis, prognosis, and treatment of cancer. miRNAs have recently been detected in human body fluids, including peripheral blood plasma as extracellular nuclease-resistant entities (Kosaka et al., 2010a). Reports in two landmark papers noted that not only mRNAs but also miRNAs were secreted outside of the cells and circulated in human body fluid (Chim et al., 2008; Lawrie et al., 2008). Chim et al. (2008) reported the existence of placental miRNAs in maternal plasma. Interestingly, they showed that the four most abundant placental miRNAs (miR-141, miR-149, miR-299-5p, and miR-135b) were detectable in maternal plasma during pregnancy and showed reduced detection rates in post-delivery plasma. Furthermore, Lawrie et al. (2008) investigated whether miRNAs have diagnostic utility by comparing the levels of tumor-associated miR-155, miR-210, and miR-21 in serum from diffuse large B-cell lymphoma patients with healthy controls and showed that the levels were higher in patients than in control sera. These observations support the idea that circulating miRNAs can be used as biomarkers to monitor an individual's health. In addition, these reports also suggest the possibility that secretory miRNA must be contained in or attached to something that could protect RNA from RNase-mediated degradation.

One breakthrough about circulating RNA was the discovery of mRNA and miRNA in exosomes (Valadi et al., 2007). Valadi et al. (2007) showed that mouse and human mast cell-derived exosomes, which are vesicles of endocytic origin released by many kinds of cells that can mediate communication between cells, contain RNA and miRNA. The RNA from mast cell exosomes is transferable to other mouse and human mast cells. After the transfer of mouse exosomal RNA to human mast cells, new mouse proteins were found in the recipient human cells, indicating that transferred exosomal mRNA can be translated after entering another cell. Observations from these three reports indicated one important fact, namely, that miRNA could be existent in the outer space of the cells, where the RNase is present, and could be functional in this new location.

After the discovery of miRNA in exosome, many researchers attempted to identify the function of secretory miRNA because the report from Valadi et al. (2007) had not clarified it in the exosomal miRNA in recipient cells. One of the earliest studies to prove the function of secretory miRNA was revealed by an apoptotic body (Zernecke et al., 2009). They demonstrated that CXCL12 production was mediated by miR-126, which was enriched in apoptotic bodies and repressed the function of the regulator of G protein signaling 16. This enabled CXCR4 to trigger an autoregulatory feedback loop that increased the production of CXCL12, leading to the recruitment of progenitor cells. This study strongly indicated the importance of a "dying message" for the regulating homeostasis of a healthy status and highlights the functions of miRNAs in health and disease that may extend to the recruitment of progenitor cells during other forms of tissue repair or homeostasis.

After the study of miRNA in apoptotic bodies, three reports showed the function and transfer of secretory miRNAs contained inside the exosome. Pegtel et al. (2010) showed that mature EBV-encoded miRNAs are secreted by EBV-infected B cells through exosomes. These EBV-miRNAs repress the EBV target immunoregulatory genes, and these target genes are down-regulated in primary EBV-associated lymphomas. Interestingly, using peripheral blood mononuclear cells from patients with an increased EBV load, these researchers also showed that, although EBV DNA is restricted to the circulating B-cell population, EBV BART miRNAs are present in both B-cell and non-B-cell fractions, suggestive of miRNA transfer *in vivo*. Zhang et al. (2010) reported that miR-150 is contained inside the exosomes and is secreted from a cultured human monocyte/macrophage cell line and that this exosome delivers miR-150 into human microvascular endothelial cells. Then, elevated exogenous miR-150 effectively reduced c-Myb expression and enhanced cell migration in human microvascular endothelial cells. Our group also demonstrated that a secreted tumor-suppressive miRNA, which is miR-146a down-regulated in prostate cancer, was transported to cancer cells and exerted gene silencing in the recipient prostate cancer cells through the suppression of its target gene, thereby leading to cell growth inhibition (Kosaka et al., 2010b). This suggested that secreted miRNA could function as a cell–cell communication tool between the cancer cells and their microenvironmental cells.

These three reports clarified a variety of physiological and pathological phenomena, including virus infection, vascular disease, and cancer. The variety of research fields highlights the importance of secretory miRNAs in phenomena vital to life. Indeed, recent reports have pointed to various functions of secretory miRNA in many aspects of life, such as cellular communication involving antigen-dependent, unidirectional intercellular transfer of miRNAs by exosomes during immune synapsis (Mittelbrunn et al., 2011), nasopharyngeal carcinoma-mediated transfer of EBV-encoded BART miRNA (Gourzones et al., 2010), hepatocellular carcinoma (Kogure et al., 2011), and cardiovascular diseases (Kuwabara et al., 2011). These reports mainly described the importance of exosomes as an miRNA carrier; however, it is not always the exosome that is important in secretory miRNA-mediated cell–cell communication.

High-density lipoprotein (HDL) transports endogenous miRNAs and delivers them to recipient cells with functional targeting capabilities (Vickers et al., 2011). The human HDL-miRNA profile of normal subjects is significantly different from that of familial hypercholesterolemia subjects. Interestingly, a recent report showed that the mechanism of horizontal transfer of miRNAs is not only dependent on vesicle transfer, such as exosomes, but

also intercellular connection tools, such as gap junction and RNA-binding protein. Lim et al. (2011) clarified that miRNA was transmitted from bone marrow stroma to breast cancer cells via gap junctions and exosomes in tumor cell quiescence. Arroyo et al. (2011) employed a technique, differential centrifugation and size-exclusion chromatography, to characterize circulating miRNA complexes in human plasma and serum and found that the majority of circulating miRNAs cofractionated with Argonaute2 (Ago2, the key effector protein of miRNA-mediated silencing) protein complexes rather than within vesicles. This study was also confirmed by other groups which have shown Ago2 (Turchinovich et al., 2011) or nucleophosmin 1 as secretory miRNA carriers (Wang et al., 2010). Further biological studies are required to understand the function of miRNAs secreted with an RNA-binding protein, such as Ago2 or nucleophosmin 1, in a variety of research fields.

To certify the significance of secretory miRNAs in variety of life phenomena, it is also essential to understand the secretion mechanism of miRNA from cells. Previously, we found in HEK293 and COS-7 cells that the secretion of miRNAs was regulated by neutral sphingomyelinase 2 (nSMase 2; Kosaka et al., 2010b), which is the catalytic enzyme of ceramide biosynthesis and is known as an exosome regulatory protein (Trajkovic et al., 2008). The decreased activity of nSMase 2 with a chemical inhibitor, GW4869, and a specific siRNA resulted in the reduced secretion of miRNAs. Complementarily, overexpression of nSMase 2 increased the extracellular amounts of miRNAs. This observation was also confirmed using other cells including T-cells (Mittelbrunn et al., 2011) and hepatocellular carcinoma cells (Kogure et al., 2011). Contrary to our results, inhibition of nSMase 2 significantly increased the amount of miRNAs exported to HDL from macrophages (Vickers et al., 2011).

It remains necessary to elucidate how miRNA is sorted into exosomes or other vesicles, such as microvesicles. Microvesicles, also known as microparticles or shedding vesicles, represent a heterogeneous population of vesicles with a diameter of 100–1000 nm that are released by budding of the plasma (Muralidharan-Chari et al., 2010). It has been shown that microvesicles isolated from embryonic stem cells increase pluripotency of hematopoietic stem cells after horizontal transfer of embryonic stem cell-derived mRNA. Although the functions of microvesicles were recently elucidated, unlike exosome, not only the function but also the sorting mechanisms of miRNAs into microvesicles have not been clarified yet. Furthermore, it has not been shown yet what kind of protein bind to miRNAs in the vesicles such as exosomes, microvesicles, and apoptotic bodies, although Arroyo et al. (2011) clearly showed that circulating Ago2-binding miRNAs were not contained inside vesicles. Gibbings et al. (2009) detected some AGO2 in the purified exosomes, albeit less than in whole-cell lysates, on the contrary, GW182, which required for miRNA function through its binding to AGO2, was dramatically enriched in exosomes. Detecting the proteins, which bind to miRNAs in vesicles, might lead to revealing the sorting mechanism of miRNAs in vesicles. Clarifying the details of the molecular mechanisms of secretory miRNA, such as the manner of cell–cell transfer or secretion mechanisms, will help us understand a variety of diseases, especially cancer (**Figure 1**).

SECRETORY miRNA AS A HUMORAL FACTOR IN CANCER CELLS

As shown in this report, secretory miRNAs are functional molecules that modulate many aspects of the biological process. In addition, destruction of the secretion of miRNA from cells might lead to disease, such as cardiovascular diseases, virus infections, deterioration of the immune system, and cancer. From the field of cancer research, we would like to propose two hypotheses regarding secretory miRNA-mediated cancer progression (**Figure 2**).

One is the function of secretory miRNA in a metastatic niche (**Figure 2A**). As already shown in several reports, various types of the cells have been shown to have the capability to take up exosomes. The tumor microenvironment is a complex tissue comprising variable numbers of tumor cells, epithelial cells which originated cancer cells, fibroblasts, endothelial cells, and infiltrating leukocytes. Recent reports have explained the mechanism of controlling the cancer cell-mediated phenotypical change of microenvironmental cells through cytokines (Hanahan and Weinberg, 2011). Cytokines are considered as key molecules controlling autocrine or paracrine communications within and between these individual cell types. However, considering the existence of secretory miRNA within these environments, their influence to the cancer niche should be reconsidered. An exosome contains nearly 300 proteins (Atay et al., 2011) with the potential to modulate the state of microenvironment cells. In addition, miRNAs are known to regulate hundreds of target mRNA expressions. Thus, not only exosomal miRNAs but also other types of secretory miRNAs could control the state of cellular phenotypes to the benefit of cancer cells within their niche.

Another hypothesis deals with the function of secretory miRNAs in distant organs (**Figure 2B**). Recently, Hood et al. (2011) provided evidence of exosome-mediated conditioning of lymph nodes and defined microanatomic responses that enable the metastasis of melanoma cells. Homing of melanoma exosomes to sentinel lymph nodes imposes synchronized molecular signals that affect melanoma cell recruitment, extracellular matrix deposition, and vascular proliferation in the lymph nodes. They showed the physiological importance of exosomes for distal metastasis; however, they have not provided evidence of the molecules species that take part in the modulation of the distal site of metastasis. To reveal the exact function of miRNA targeting sites that are distant from the primary organ, we should identify the molecular mechanisms of the tropism of secretory miRNA transported by carriers.

SECRETORY miRNA AS A HUMORAL FACTOR IN ORGANISMS

In this study, systemic transfer of miRNAs has been introduced. However, an active mechanism for the transport of double strand RNA (dsRNA) across tissues and cellular boundaries was found in other organisms, such as nematode and plant. Transmembrane channel-forming protein SID-1 has been shown to mediate passive cellular uptake and cell-to-cell distribution of dsRNA in the nematode *C. elegans* (Feinberg and Hunter, 2003). In addition, recent report showed that mammalian SID-1 homolog localized to the cell membrane of human cells enhances their uptake of small interfering RNA, resulting in increased siRNA-mediated gene silencing efficacy (Duxbury et al., 2005). Furthermore, although RNA molecules have been implicated in systemic cell-to-cell communication

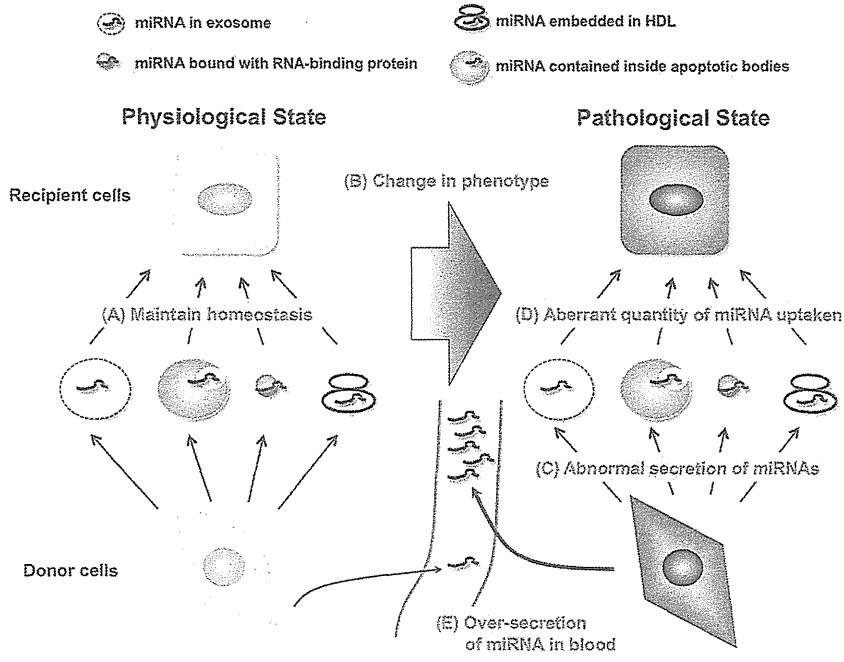

FIGURE 1 | Unveiling the mechanisms and roles of secretory miRNAs in both physiological and pathological conditions is essential for the development of novel diagnostic methods and therapeutics to treat various human diseases. In the physiological condition, secretory miRNAs may maintain the homeostasis of organs and tissues *via* diverse types of miRNA carriers **(A)**. However, this state may be destroyed by the change of phenotype in donor cells or recipient cells **(B)**. From the viewpoint of donor cells, changes in the phenotype of donor cells may lead to the alteration of miRNA species with carriers **(C)**. Furthermore, the quantity of secretory miRNA uptake by recipient cells may change in this situation **(D)**. It is necessary to understand these abnormal changes of molecular mechanisms for the development of a therapy against "secretory miRNAs-mediated diseases." In addition, it is possible that the amount of secretory miRNAs changes in this situation through the abnormal regulation of carrier production **(E)**. Understanding these changes may lead to the exploitation of a diagnosis marker for "secretory miRNAs-mediated diseases."

in plants (Chitwood and Timmermans, 2010), recent studies have shown that miRNAs are mobile signals that control gene expression during plant development (Dunoyer et al., 2010; Molnar et al., 2010), suggesting that the transfer of RNA is found globally in organisms.

Surprisingly, Zhang et al. (2011) reported that exogenous plant miRNAs are present in the sera and tissues of various animals and that these exogenous plant miRNAs are primarily acquired orally, through food intake. Rice abundant miRNA, miR-168a, is one of the most highly enriched exogenous plant miRNAs in the sera of Chinese subjects. Furthermore, they also found that MIR168a could bind to the human/mouse low-density lipoprotein receptor adapter protein 1 (LDLRAP1) mRNA, inhibit LDLRAP1 expression in liver, and consequently decrease LDL removal from mouse plasma. This study prompted the idea that miRNAs could regulate the gene expression across the kingdom. In addition, one of the important point of this study is that identification of plant miRNAs in human peripheral blood was performed by Solexa sequencing. High-throughput transcriptome analysis by Next Generation Sequencing, specifically RNAseq, is currently widely available. As shown in the case of rice miRNAs, these techniques may help answer the question about the novel small RNAs recently discovered to be secreted.

FUTURE DIRECTIONS FOR RESEARCH ON SECRETORY RNAs

In this review, we summarized the recent findings of secretory miRNAs. The research field of secretory miRNAs has just begun. To use the knowledge of secretory miRNAs for human health, we should unveil the mystery of secretory RNA as follows.

First, we need to know the all kinds of secretory RNA species. Interestingly, Dinger et al. (2008) independently analyzed the microarray dataset from Valadi et al.'s (2007) study and found that many longer non-coding RNAs (ncRNAs) were also present in exosomes, including a number of ncRNAs associated with important genes and several known ncRNAs, such as Copg2as and Nespas, in mast cell-derived exosomes. This question seems quite easy to obtain the answer. As we already mentioned above, recent development of next generation sequencing technologies has been developed. This means that we can directly recognize the nucleic acids that can exist outer space of the cells.

Second, secretory machinery of miRNAs and other types of RNA should be clarified. As described in this paper, we recently detected the part of miRNAs secretion mechanism mediated by exosome (Kosaka et al., 2010b). Analyzing the secretion mechanism of various kinds of RNAs and sorting mechanism of miRNA into the vesicles leads the development of novel nucleic acids based medicine.

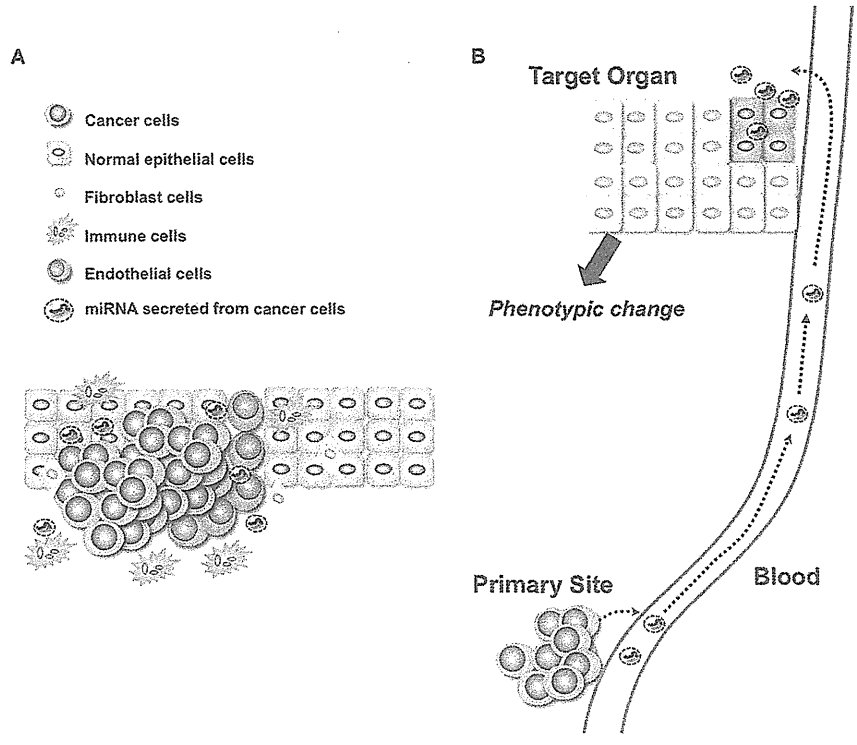

FIGURE 2 | Two proposed hypotheses regarding secretory miRNA-mediated cancer progression. (A) Secretory miRNAs mediate the modulation of microenvironmental cells. Secretory miRNAs from cancer cells control the behavior of microenvironmental cells for their own benefit. **(B)** Secretory miRNAs could be functional molecules in a distant organ.

Last point is to know the function of secretory miRNAs in more detail, such as physiological conditions and pathological conditions. Reports on the function of secretory miRNAs in physiological conditions, such as embryogenesis, organogenesis, and maintaining tissue and organ homeostasis, are not available. In addition, to know the function of secretory miRNAs, we need to know the incorporation mechanism of miRNAs. Although SID-1 found in *C. elegans* is good example of secretory miRNA transport mechanism, the other machinery might exist in vertebrates. Indeed, both transporter-dependent (SID-1 dependent) and transporter-independent (SID-1 independent) dsRNA export takes place from *C. elegans* cells (Jose et al., 2009). Furthermore, as shown previously, miRNA from plant was detected in human circulating peripheral blood, and the function of plant derived miRNA was documented by the authors, suggesting that other types of small RNA from other species might contribute to the regulating of physiological or pathological situation. Because miRNAs act as multi-functional molecules via the binding to sequence similarities and regulate various life phenomena, secretory miRNAs might be a humoral factor that exerts its influence in distant organs, similarly to hormones. Clarifying the species, mechanisms and roles of secretory miRNA, and other secretory ncRNAs in both pathological and physiological conditions would unveil the mystery of "secretory miRNAs-mediated disease" (**Figure 1**).

ACKNOWLEDGMENTS

This work was supported in part by a grant-in-aid for the Third-Term Comprehensive 10-Year Strategy for Cancer Control, a grant-in-aid for Scientific Research on Priority Areas Cancer from the Ministry of Education, Culture, Sports, Science, and Technology, the Program for Promotion of Fundamental Studies in Health Sciences of the National Institute of Biomedical Innovation, and the Japan Society for the Promotion of Science through the "Funding Program for World-Leading Innovative R&D on Science and Technology (FIRST Program)" initiated by the Council for Science and Technology Policy. We apologize to colleagues whose work we could not cite owing to space limitations. We are grateful for Dr. Nami Nogawa-Kosaka for critical reading of the manuscript.

REFERENCES

Arroyo, J. D., Chevillet, J. R., Kroh, E. M., Ruf, I. K., Pritchard, C. C., Gibson, D. F., Mitchell, P. S., Bennett, C. F., Pogosova-Agadjanyan, E. L., Stirewalt, D. L., Tait, J. F., and Tewari, M. (2011). Argonaute2 complexes carry a population of circulating microRNAs independent of vesicles in human plasma. *Proc. Natl. Acad. Sci. U.S.A.* 108, 5003–5008.

Atay, S., Gercel-Taylor, C., Kesimer, M., and Taylor, D. D. (2011). Morphologic and proteomic characterization of exosomes released by cultured extravillous trophoblast cells. *Exp. Cell Res.* 317, 1192–1202.

Chim, S. S., Shing, T. K., Hung, E. C., Leung, T. Y., Lau, T. K., Chiu, R. W., and Lo, Y. M. (2008). Detection and characterization of placental microRNAs in maternal plasma. *Clin. Chem.* 54, 482–490.

Chitwood, D. H., and Timmermans, M. C. (2010). Small RNAs are on the move. *Nature* 467, 415–419.

Dinger, M. E., Mercer, T. R., and Mattick, J. S. (2008). RNAs as extracellular signaling molecules. *J. Mol. Endocrinol.* 40, 151–159.

Dunoyer, P., Schott, G., Himber, C., Meyer, D., Takeda, A., Carrington, J. C., and Voinnet, O. (2010). Small RNA duplexes function as mobile silencing signals between plant cells. *Science* 328, 912–916.

Duxbury, M. S., Ashley, S. W., and Whang, E. E. (2005). RNA interference: a mammalian SID-1 homologue enhances siRNA uptake and gene silencing efficacy in human cells. *Biochem. Biophys. Res. Commun.* 3, 459–463.

Feinberg, E. H., and Hunter, C. P. (2003). Transport of dsRNA into cells by the transmembrane protein SID-1. *Science* 12, 1545–1547.

Fleischhacker, M., and Schmidt, B. (2007). Circulating nucleic acids (CNAs) and cancer – a survey. *Biochim. Biophys. Acta* 1775, 181–232.

Galand, P., and Ledoux, L. (1966). Uptake of exogenous ribonucleic acid by ascites tumor cells. II. Relations between RNA uptake and the cellular metabolism. *Exp. Cell Res.* 43, 391–397.

Garzon, R., Marcucci, G., and Croce, C. M. (2010). Targeting microRNAs in cancer: rationale, strategies and challenges. *Nat. Rev. Drug Discov.* 9, 775–789.

Gibbings, D. J., Ciaudo, C., Erhardt, M., and Voinnet, O. (2009). Multivesicular bodies associate with components of miRNA effector complexes and modulate miRNA activity. *Nat. Cell Biol.* 11, 1143–1149.

Gourzones, C., Gelin, A., Bombik, I., Klibi, J., Verillaud, B., Guigay, J., Lang, P., Temam, S., Schneider, V., Amiel, C., Baconnais, S., Jimenez, A. S., and Busson, P. (2010). Extracellular release and blood diffusion of BART viral micro-RNAs produced by EBV-infected nasopharyngeal carcinoma cells. *Virol. J.* 7, 271.

Hanahan, D., and Weinberg, R. A. (2011). Hallmarks of cancer: the next generation. *Cell* 144, 646–674.

Hood, J. L., San, R. S., and Wickline, S. A. (2011). Exosomes released by melanoma cells prepare sentinel lymph nodes for tumor metastasis. *Cancer Res.* 71, 3792–3801.

Jose, A. M., Smith, J. J., and Hunter, C. P. (2009). Export of RNA silencing from *C. elegans* tissues does not require the RNA channel SID-1. *Proc. Natl. Acad. Sci. U.S.A.* 106, 2283–2288.

Kogure, T., Lin, W. L., Yan, I. K., Braconi, C., and Patel, T. (2011). Intercellular nanovesicle-mediated microRNA transfer: a mechanism of environmental modulation of hepatocellular cancer cell growth. *Hepatology* 54, 1237–1248.

Kolodny, G. M. (1971). Evidence for transfer of macromolecular RNA between mammalian cells in culture. *Exp. Cell Res.* 65, 313–324.

Kosaka, N., Iguchi, H., and Ochiya, T. (2010a). Circulating microRNA in body fluid: a new potential biomarker for cancer diagnosis and prognosis. *Cancer Sci.* 101, 2087–2092.

Kosaka, N., Iguchi, H., Yoshioka, Y., Takeshita, F., Matsuki, Y., and Ochiya, T. (2010b). Secretory mechanisms and intercellular transfer of microRNAs in living cells. *J. Biol. Chem.* 285, 17442–17452.

Kuwabara, Y., Ono, K., Horie, T., Nishi, H., Nagao, K., Kinoshita, M., Watanabe, S., Baba, O., Kojima, Y., Shizuta, S., Imai, M., Tamura, T., Kita, T., and Kimura, T. (2011). Increased microRNA-1 and microRNA-133a levels in serum of patients with cardiovascular disease indicate the existence of myocardial damage. *Circ. Cardiovasc. Genet.* 4, 446–454.

Kwak, P. B., Iwasaki, S., and Tomari, Y. (2011). The microRNA pathway and cancer. *Cancer Sci.* 101, 2309–2315.

Lawrie, C. H., Gal, S., Dunlop, H. M., Pushkaran, B., Liggins, A. P., Pulford, K., Banham, A. H., Pezzella, F., Boultwood, J., Wainscoat, J. S., Hatton, C. S., and Harris, A. L. (2008). Detection of elevated levels of tumour-associated microRNAs in serum of patients with diffuse large B-cell lymphoma. *Br. J. Haematol.* 141, 672–675.

Lim, P. K., Bliss, S. A., Patel, S. A., Taborga, M., Dave, M. A., Gregory, L. A., Greco, S. J., Bryan, M., Patel, P. S., and Rameshwar, P. (2011). Gap junction-mediated import of microRNA from bone marrow stromal cells can elicit cell cycle quiescence in breast cancer cells. *Cancer Res.* 71, 1550–1560.

Mandel, P., and Metais, P. (1947). Les acides nucleiques du plasma sanguin chez l'homme. *C. R. Acad. Sci. Paris* 142, 241–243.

Mittelbrunn, M., Gutierrez-Vazquez, C., Villarroya-Beltri, C., Gonzalez, S., Sanchez-Cabo, F., Gonzalez, M. A., Bernad, A., and Sanchez-Madrid, F. (2011). Unidirectional transfer of microRNA-loaded exosomes from T cells to antigen-presenting cells. *Nat. Commun.* 2, 282.

Molnar, A., Melnyk, C. W., Bassett, A., Hardcastle, T. J., Dunn, R., and Baulcombe, D. C. (2010). Small silencing RNAs in plants are mobile and direct epigenetic modification in recipient cells. *Science* 328, 872–875.

Muralidharan-Chari, V., Clancy, J. W., Sedgwick, A., and D'Souza-Schorey, C. (2010). Microvesicles: mediators of extracellular communication during cancer progression. *J. Cell. Sci.* 15, 1603–1611.

Pegtel, D. M., Cosmopoulos, K., Thorley-Lawson, D. A., Van Eijndhoven, M. A., Hopmans, E. S., Lindenberg, J. L., De Gruijl, T. D., Wurdinger, T., and Middeldorp, J. M. (2010). Functional delivery of viral miRNAs via exosomes. *Proc. Natl. Acad. Sci. U.S.A.* 107, 6328–6333.

Reddi, K. K., and Holland, J. F. (1976). Elevated serum ribonuclease in patients with pancreatic cancer. *Proc. Natl. Acad. Sci. U.S.A.* 73, 2308–2310.

Rieber, M., and Bacalao, J. (1974). An "external" RNA removable from mammalian cells by mild proteolysis. *Proc. Natl. Acad. Sci. U.S.A.* 71, 4960–4964.

Stroun, M., Anker, P., Beljanski, M., Henri, J., Lederrey, C., Ojha, M., and Maurice, P. A. (1978). Presence of RNA in the nucleoprotein complex spontaneously released by human lymphocytes and frog auricles in culture. *Cancer Res.* 38, 3546–3554.

Trajkovic, K., Hsu, C., Chiantia, S., Rajendran, L., Wenzel, D., Wieland, F., Schwille, P., Brugger, B., and Simons, M. (2008). Ceramide triggers budding of exosome vesicles into multivesicular endosomes. *Science* 319, 1244–1247.

Tsui, N. B., Ng, E. K., and Lo, Y. M. (2002). Stability of endogenous and added RNA in blood specimens, serum, and plasma. *Clin. Chem.* 48, 1647–1653.

Turchinovich, A., Weiz, L., Langheinz, A., and Burwinkel, B. (2011). Characterization of extracellular circulating microRNA. *Nucleic Acids Res.* 39, 7223–7233.

Valadi, H., Ekstrom, K., Bossios, A., Sjostrand, M., Lee, J. J., and Lotvall, J. O. (2007). Exosome-mediated transfer of mRNAs and microRNAs is a novel mechanism of genetic exchange between cells. *Nat. Cell Biol.* 9, 654–659.

Vickers, K. C., Palmisano, B. T., Shoucri, B. M., Shamburek, R. D., and Remaley, A. T. (2011). MicroRNAs are transported in plasma and delivered to recipient cells by high-density lipoproteins. *Nat. Cell Biol.* 13, 423–433.

Wang, K., Zhang, S., Weber, J., Baxter, D., and Galas, D. J. (2010). Export of microRNAs and microRNA-protective protein by mammalian cells. *Nucleic Acids Res.* 38, 7248–7259.

Watson, J. D., and Crick, F. H. (1953). Molecular structure of nucleic acids; a structure for deoxyribose nucleic acid. *Nature* 171, 737–738.

Wieczorek, A. J., Sitaramam, V., Machleidt, W., Rhyner, K., Perruchoud, A. P., and Block, L. H. (1987). Diagnostic and prognostic value of RNA-proteolipid in sera of patients with malignant disorders following therapy: first clinical evaluation of a novel tumor marker. *Cancer Res.* 47, 6407–6412.

Zernecke, A., Bidzhekov, K., Noels, H., Shagdarsuren, E., Gan, L., Denecke, B., Hristov, M., Koppel, T., Jahantigh, M. N., Lutgens, E., Wang, S., Olson, E. N., Schober, A., and Weber, C. (2009). Delivery of microRNA-126 by apoptotic bodies induces CXCL12-dependent vascular protection. *Sci. Signal.* 2, ra81.

Zhang, L., Hou, D., Chen, X., Li, D., Zhu, L., Zhang, Y., Li, J., Bian, Z., Liang, X., Cai, X., Yin, Y., Wang, C., Zhang, T., Zhu, D., Zhang, D., Xu, J., Chen, Q., Ba, Y., Liu, J., Wang, Q., Chen, J., Wang, J., Wang, M., Zhang, Q., Zhang, J., Zen, K., and Zhang, C. Y. (2011). Exogenous plant MIR168a specifically targets mammalian LDLRAP1: evidence of cross-kingdom regulation by microRNA. *Cell Res.* PMID: 21931358. [Epub ahead of print].

Zhang, Y., Liu, D., Chen, X., Li, J., Li, L., Bian, Z., Sun, F., Lu, J., Yin, Y., Cai, X., Sun, Q., Wang, K., Ba, Y., Wang, Q., Wang, D., Yang, J., Liu, P., Xu, T., Yan, Q., Zhang, J., Zen, K., and Zhang, C. Y. (2010). Secreted monocytic miR-150 enhances targeted endothelial cell migration. *Mol. Cell* 39, 133–144.

Conflict of Interest Statement: The authors declare that the research was conducted in the absence of any commercial or financial relationships that could be construed as a potential conflict of interest.

Received: 29 August 2011; paper pending published: 20 September 2011; accepted: 08 December 2011; published online: 03 January 2012.

Citation: Kosaka N and Ochiya T (2012) Unraveling the mystery of cancer by secretory microRNA: horizontal microRNA transfer between living cells. Front. Gene. 2:97. doi: 10.3389/fgene.2011.00097

This article was submitted to Frontiers in Non-Coding RNA, a specialty of Frontiers in Genetics.

Copyright © 2012 Kosaka and Ochiya. This is an open-access article distributed under the terms of the Creative Commons Attribution Non Commercial License, which permits non-commercial use, distribution, and reproduction in other forums, provided the original authors and source are credited.

© The American Society of Gene & Cell Therapy

Systemically Injected Exosomes Targeted to EGFR Deliver Antitumor MicroRNA to Breast Cancer Cells

Shin-ichiro Ohno[1], Masakatsu Takanashi[1], Katsuko Sudo[2], Shinobu Ueda[1], Akio Ishikawa[1], Nagahisa Matsuyama[1], Koji Fujita[1], Takayuki Mizutani[1], Tadaaki Ohgi[3], Takahiro Ochiya[4], Noriko Gotoh[5] and Masahiko Kuroda[1]

[1]Department of Molecular Pathology, Tokyo Medical University, Tokyo, Japan; [2]Animal Research Center, Tokyo Medical University, Tokyo, Japan; [3]BONAC Corporation, Fukuoka BIO Factory 4F, Fukuoka, Japan; [4]Division of Molecular and Cellular Medicine, National Cancer Center Research Institute, Tokyo, Japan; [5]Division of Systems Biomedical Technology, Institute of Medical Science, University of Tokyo, Tokyo, Japan

Despite the therapeutic potential of nucleic acid drugs, their clinical application has been limited in part by a lack of appropriate delivery systems. Exosomes or microvesicles are small endosomally derived vesicles that are secreted by a variety of cell types and tissues. Here, we show that exosomes can efficiently deliver microRNA (miRNA) to epidermal growth factor receptor (EGFR)-expressing breast cancer cells. Targeting was achieved by engineering the donor cells to express the transmembrane domain of platelet-derived growth factor receptor fused to the GE11 peptide. Intravenously injected exosomes delivered let-7a miRNA to EGFR-expressing xenograft breast cancer tissue in RAG2$^{-/-}$ mice. Our results suggest that exosomes can be used therapeutically to target EGFR-expressing cancerous tissues with nucleic acid drugs.

Received 17 March 2012; accepted 1 August 2012; advance online publication 2 October 2012. doi:10.1038/mt.2012.180

INTRODUCTION

MicroRNAs (miRNAs) are small (20–22 nucleotides) noncoding RNA molecules that bind to partially complementary mRNA sequences, resulting in target degradation or translation inhibition.[1] A growing pool of evidence suggests that miRNA-related gain- or loss-of-function mutations can cause the development and/or progression of cancer.[2] For example, let-7a is thought to be a tumor suppressor that inhibits the malignant growth of cancer cells by reducing RAS and HMGA2 expression. Reduced expression levels of let-7 have been observed in colon, lung, ovary, and breast cancer cells.[3] Therefore, miRNA replacement therapies have emerged as promising treatment strategies for malignant neoplasms. Yet although miRNA-based modalities may eventually prove effective, their clinical application has been hampered by a lack of appropriate delivery systems.

Exosomes or microvesicles are small vesicles (50–100 nm in diameter) that are secreted by a variety of cell types and tissues.[4] Of clinical interest, tumor cells have been shown to release exosomes containing miRNA[5] and miRNAs secreted from donor cells can be taken up and function in recipient cells.[6,7] These data indicate that exosomes are natural carriers of miRNA that could be exploited as an RNA drug delivery system. For instance, Alvarez-Erviti *et al.* recently used exosomes with modified membranes containing a neuron-specific peptide to deliver small-interfering RNA (siRNA) to mouse brain tissue.[8] Nevertheless, the utility of exosomes as carriers of cancer therapies remains largely unknown.

A number of human tumors of epithelial origin display elevated epidermal growth factor receptor (EGFR) expression, suggesting that EGFR could serve as a receptor target in cancer drug delivery systems.[9] Because the EGFR ligand epidermal growth factor (EGF) is strongly mitogenic and neoangiogenic, however, an alternative ligand is needed for clinical applications.

The GE11 peptide (amino-acid sequence YHWYGYTPQNVI) binds specifically to EGFR, but is markedly less mitogenic than EGF.[10] Additionally, GE11-conjugated polyethylenimine vectors and polyethylene glycol–conjugated liposomes have been shown to be less mitogenic, and can efficiently transfect genes into cells expressing high levels of EGFR or tumor xenografts.[10–13] These studies indicated that the GE11 peptide is likely superior to EGF for clinically targeting EGFR-expressing tumors.

In this study, we examined exosomes as drug delivery carriers in a model of cancer. Modified exosomes with the GE11 peptide or EGF on their surfaces delivered miRNA to EGFR-expressing cancer tissues; intravenously injected exosomes targeting EGFR delivered let-7a specifically to xenograft breast cancer cells in RAG2$^{-/-}$ mice. These data indicate that exosomes targeted to EGFR-expressing cells may provide a platform for miRNA replacement therapies in the treatment of various cancers.

RESULTS

GE11- and EGF-positive exosomes

GE11 peptide specifically binds to EGFR, but is less mitogenic than EGF.[10] To generate GE11- or EGF-positive exosomes, sequence encoding GE11 or EGF was cloned into the pDisplay vector. This vector promotes the expression of proteins on plasma membranes

Correspondence: Masahiko Kuroda, Department of Molecular Pathology, Tokyo Medical University, 6-1-1 Shinjuku, Shinjuku-ku, Tokyo 160-8402, Japan. E-mail: kuroda@tokyo-med.ac.jp

© The American Society of Gene & Cell Therapy

using the transmembrane domain of platelet-derived growth factor receptor (**Figure 1a**). We transfected human embryonic kidney cell line 293 (HEK293) cells with pDisplay encoding GE11 or EGF, and then cloned cells that were stably expressing the constructs. Exosomes were purified from culture supernatants using an ultracentrifugation protocol (see Materials and Methods section).

We then examined the expression of GE11 or EGF in exosomes using anti-hemagglutinin (HA) antibodies and western blot analysis, which revealed bands of the predicted sizes (**Figure 1b**). In addition, fluorescence-activated cell sorting (FACS) confirmed the presence of GE11 and EGF on the outer membranes of exosomes bound to latex beads, and these complexes were recognized by anti-Myc-tag antibodies (**Figure 1c**). CD81 was used as a positive control for exosomes. Myc-tag expression was observed more

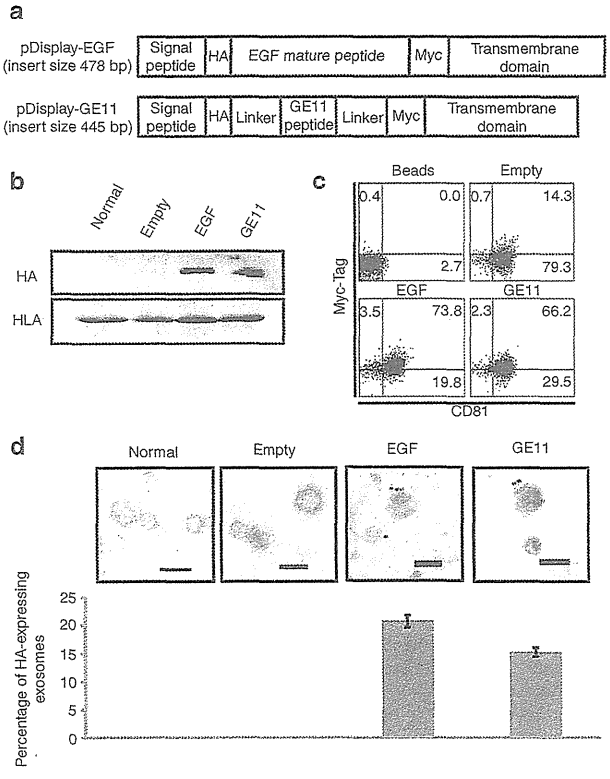

Figure 1 Epidermal growth factor receptor (EGFR) ligands on the outer surfaces of the exosomes. (**a**) Diagrams of the modified epidermal growth factor (EGF) and GE11 proteins. Signal peptide, Igκ-chain leader sequence; HA, hemagglutinin epitope tag (YPYDVPDYA); Linker, (GGGGS) 3; Myc, Myc epitope (EEKLISEEDL); platelet-derived growth factor receptor (PDGFR) transmembrane domain, transmembrane domain from platelet-derived growth factor receptor. (**b**) Western blots of HA-tagged constructs in exosomes obtained from culture supernatants of human embryonic kidney cell line 293 (HEK293) cells that had been transfected with pDisplay encoding EGF or GE11. The quality of each exosome preparation was confirmed by hybridization with antihuman leukocyte antigen (HLA) antibodies. (**c**) For flow cytometry, exosomes from transfected HEK293 cells were incubated with latex beads and stained with anti-Myc tag antibodies. Tetraspanin CD81 was used as a positive control for the exosomes. (**d**) Immunoelectron microscopy showed that HA-tagged constructs were present on exosomes purified from the supernatants of cells transfected with pDisplay encoding EGF or GE11. Bars = 100 nm. The percentages of HA-positive exosomes are indicated in the graph. Data are expressed as means ± SD.

frequently in EGF-positive (73.8%) and GE11-positive (66.2%) exosomes than in vector control (14.3%) exosomes. These data indicated that GE11 or EGF was present on the exosomal membranes. Additionally, immunogold staining with anti-HA antibodies showed that 15.3% and 21.2% of the exosomes were positive for GE11 and EGF, respectively, and no notable morphologic abnormalities were observed in the modified exosomes (**Figure 1d**).

EGFR-dependent uptake of modified exosomes *in vitro*

We next examined whether the GE11- or EGF-positive exosomes derived from HEK293 cells bound to recipient cells in an EGFR-dependent manner. We first evaluated EGFR expression in three human breast cancer cell lines. HCC70 cells showed higher EGFR expression levels than HCC1954 and MCF-7 cells (**Figure 2a**). To examine whether GE11- or EGF-positive exosomes were taken up by recipient cells, exosomes were labeled with PKH67 dye (green) and added to cultures of HCC70 cells (**Figure 2b**). EGF- and GE11-positive exosomes more efficiently bound to HCC70 cells than HCC1954 or MCF-7 cells. Binding appeared to reflect EGFR expression levels (**Figure 2b**). Exosomes did not bind to cell surface membranes when the samples were incubated at 4 °C, suggesting that the cells had to be biologically active (**Figure 2b**). Confocal laser-scanning microscopy demonstrated that the exosomes were internalized by the cells (**Figure 2c**). To confirm that EGF- and GE11-positive exosomes were taken up by an EGFR-dependent mechanism, we performed assays using breast cancer cell lines with different levels of EGFR expression. First, we prepared MCF-7 cells expressing high levels of EGFR using a retroviral vector (**Figure 2d**) and examined uptake of EGF- and GE11-positive exosomes (**Figure 2e**). EGF- and GE11-positive exosomes showed high affinities for these MCF-7 cells compared with cells infected with empty vector or untreated cells. Next, we prepared HCC70 cells in which EGFR expression was knocked down using siRNA. Three days post-transfection, EGFR expression was markedly reduced, and we examined exosome uptake using fluorescence-activated cell sorting analysis (**Figure 2f**). Because the cells proliferated following transfection of EGFR siRNA, relatively low levels of siRNA were detected in PKH67-labeled exosomes compared with the experiment shown in **Figure 2b**. Of note, however, siRNA levels decreased to near background levels in HCC70 cells in which EGFR expression was reduced compared with cells expressing high levels of EGFR or cells transfected with nontarget siRNA.

To assess whether EGF- or GE11-positive exosomes affected cell growth *in vitro*, we performed cell proliferation assays using HCC70 cells. EGF-positive exosomes promoted cell proliferation, whereas no effect was noted with control or GE11-positive exosomes (**Supplementary Figure S1**). These experiments suggested that, unlike EGF-positive exosomes, GE11-positive exosomes do not stimulate EGFR signaling. Thus, GE11-positive exosomes may provide a more suitable drug delivery system than EGF-positive exosomes.

GE11-positive exosomes are functional *in vitro*

Our results indicated that the modified exosomes were taken up into recipient cells. Next, we investigated exosome-mediated delivery of siRNA or miRNA *in vivo*, including the effects of the exogenous siRNA or miRNA in the recipient cells. We first

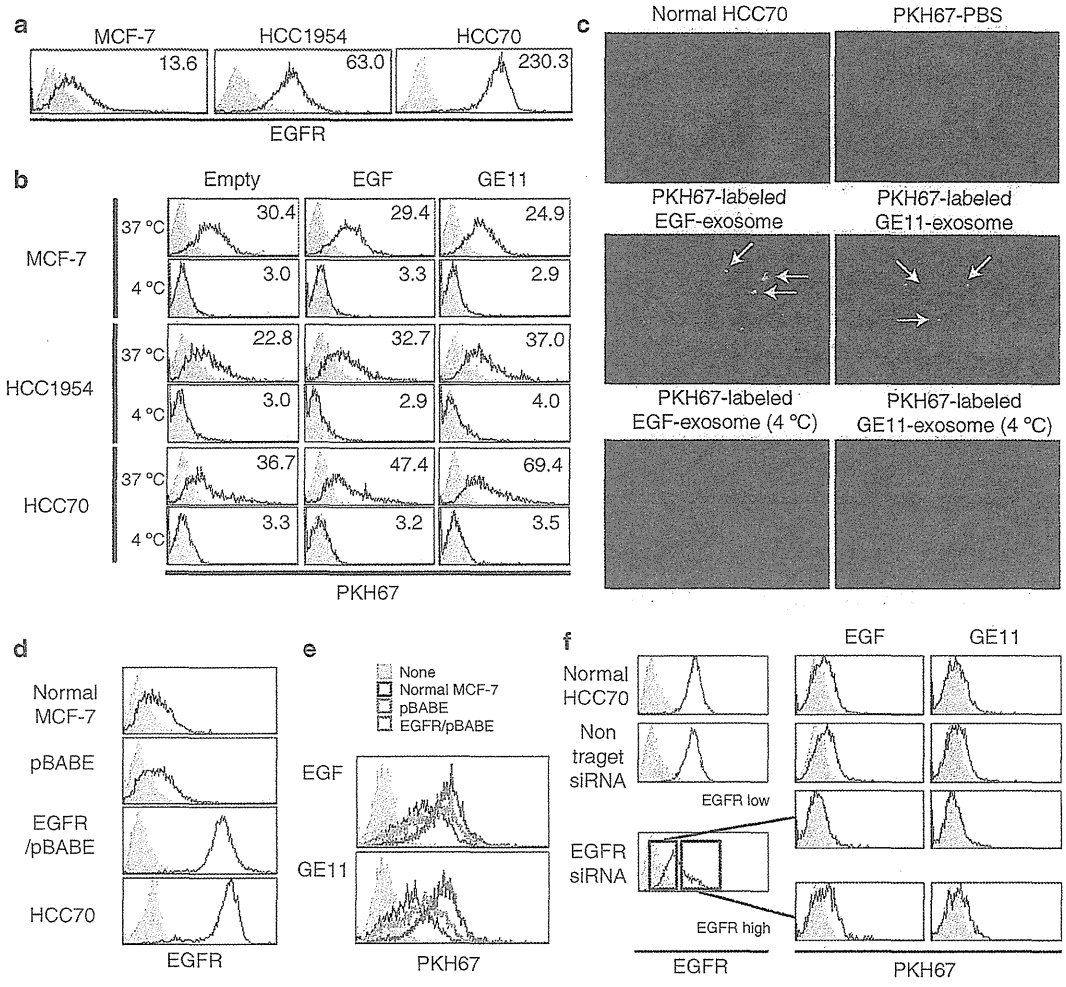

Figure 2 Uptake of epidermal growth factor (EGF)- and GE11-positive exosomes by breast cancer cell lines. (**a**) Flow cytometric analysis of epidermal growth factor receptor (EGFR) expression on HCC70, HCC1954, and MCF-7 breast cancer cells. (**b**) Uptake of fluorescently labeled exosomes by the breast cancer cell lines was detected using flow cytometry. PKH67-labeled exosomes were incubated with the breast cancer cell lines at 37 °C or 4 °C for 4 hours. The degree of uptake was relatively low at 4 °C. (**c**) Intracellular PKH67-labeled exosomes were detected in HCC70 cells (arrows) using confocal fluorescence microscopy. (**d**) Flow cytometric analysis of EGFR expression on MCF-7 cells, which were stably infected with retrovirus expressing EGFR. (**e**) Uptake of PKH67-labeled EGF- and GE11-positive exosomes was compared using MCF-7 cells expressing high levels of EGFR and control cells. (**f**) Uptake of PKH67-labeled EGF- and GE11-positive exosomes was compared among $EGFR^{Low}$ HCC70, $EGFR^{High}$, and control cells.

transfected HEK293 cells with luciferase-specific siRNA and purified loaded exosomes. Then, we added the exosomes to culture medium containing luciferase-expressing HCC70 cells. After 24 hours, we measured luciferase activities and found that GE11-positive exosomes containing luciferase-specific siRNA reduced luciferase activity in the cells (**Figure 3**). These exosomes likely contained only a fraction of the transfected siRNA from the exosome-secreting cells. Nevertheless, the encapsulated siRNA significantly inhibited expression of the target luciferase gene.

GE11-positive exosomes bind tumor cells *in vivo*

We then examined whether GE11-positive exosomes specifically bind to tumors *in vivo*. Luciferase-expressing HCC70 cells were transplanted into the mammary fat pads of $RAG2^{-/-}$ mice. GE11-positive and control exosomes were labeled with XenoLight DiR and intravenously injected into tumor-bearing $RAG2^{-/-}$ mice via the tail vein. Twenty-four hours later, the locations of the exosomes were monitored using an *in vivo* imaging system (IVIS). Signals from the GE11-positive exosomes were detected in the xenograft tumors, whereas little signal was detected in experiments using control exosomes (**Figure 4a**). We also counted the exosomes and observed that, compared with control exosomes, three times as many GE11-positive exosomes reached the tumor (**Figure 4b**). In addition, we did not histologically detect any major organ damage in the injected mice (**Supplementary Figure S2**). These data indicated that GE11-positive exosomes may facilitate the delivery of therapeutic molecules to EGFR-expressing tumors *in vivo*.

GE11-positive exosomes containing let-7 inhibit tumor development *in vivo*

We next investigated the delivery of miRNA to tumors using the GE11-positive exosomes. We used let-7a because elevated

© The American Society of Gene & Cell Therapy

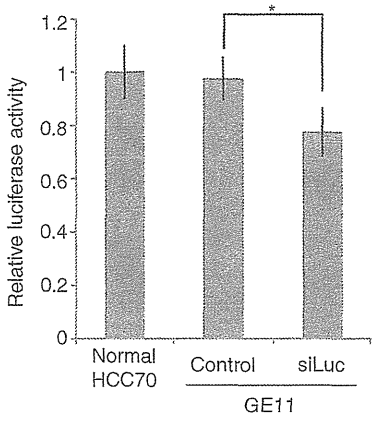

Figure 3 The activity of encapsulated small-interfering RNA (siRNA) in luciferase assays. Luciferase-specific siRNA (siLuc) was encapsulated in exosomes, which were incubated for 48 hours with HCC70 cells stably expressing firefly luciferase. Data are expressed as means ± SD. $n = 3$; $^*P < 0.05$.

let-7 expression in cancer cell lines alters cell cycle progression and reduces cell division, suggesting that let-7 functions as a tumor suppressor.[14,15] Let-7a or control miRNA was introduced into GE11-positive or control exosomes using the lipofection method and HEK293 cells, and the amount of loaded miRNA was determined in quantitative real-time reverse transcription-PCRs (**Figure 5a**). To measure tumor growth in RAG2$^{-/-}$ mice, we prepared tumor-bearing mice with xenograft HCC70 cells that stably expressed luciferase. To analyze tumor growth and development, we injected the tumors with luciferin and monitored signal emission using an IVIS. Exosomes were intravenously injected into tumor-bearing mice via the tail vein. After four injections, tumor growth was measured. Let-7a–containing GE11-positive exosomes markedly suppressed tumor growth (**Figure 5b** and **c**; $n = 6$, $P < 0.01$). Several studies have reported that let-7a inhibits tumor development by reducing expression levels of HMGA2 or members of the RAS family (K-RAS, H-RAS, N-RAS).[16] We examined the expression of these genes in let-7a–transfected HCC70 cells using real-time reverse transcription-PCR analysis, immunoblotting, and immunostaining (**Supplementary Figure S3a–c**). Furthermore, we immunohistochemically assessed the expression of HMGA2 and RAS family members in xenograft tumors (**Supplementary Figure S3d**). Let-7a did not affect the expression of HMGA2 or RAS family members *in vivo* or *in vitro*. Consistent with previous reports, however, let-7a potently inhibited the expression of HMGA2 mRNA in A549 lung adenocarcinoma cells[17] (**Supplementary Figure S3a**). These data indicated that let-7a inhibits tumor development via previously unidentified or uncharacterized genes in HCC70 breast cancer cells. Taken together, these findings indicated that GE11-positive exosomes are a promising vehicle for delivering drugs to EGFR-expressing tumors.

DISCUSSION

Although miRNA is a promising anticancer therapeutic modality, the clinical use of these RNA molecules has been hampered by a lack of malignant tissue–specific delivery systems. In the present

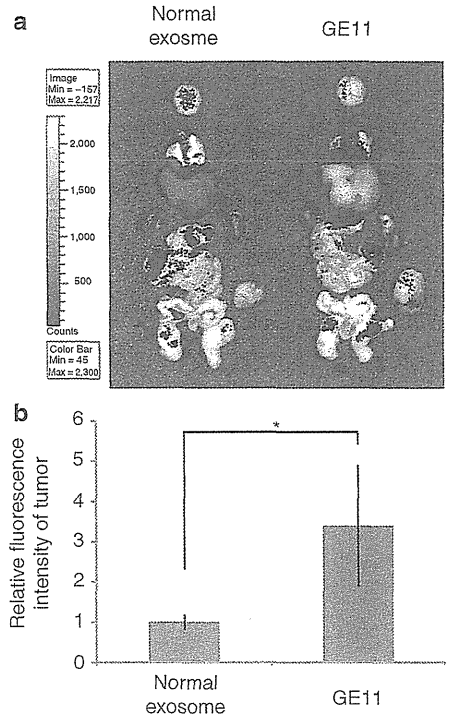

Figure 4 Migration of GE11-positive exosomes to tumor tissues characterized by high levels of epidermal growth factor receptor (EGFR) expression. (**a**) Exosomes labeled with XenoLight DiR (near-infrared) were intravenously injected (4 µg of purified exosomes) into mice bearing transplanted HCC70 cells. Brain, heart, spleen, liver, lung, kidney, small intestine, colon, and tumor tissues were harvested 24 hours postinjection for *ex vivo* imaging. The migration of fluorescently labeled exosomes was detected with an *in vivo* imaging system (IVIS). (**b**) The intensity of fluorescent signals from the tumor was measured using an IVIS. Data are expressed as means ± SD. $n = 5$; $^*P < 0.05$.

study, we showed that exosomes can be used to efficiently deliver antitumor miRNA to cancer tissues *in vivo*.

A number of nanocarriers using various materials have been developed for drug delivery systems. Polyethylene glycol–coated liposomes, which are frequently used as carriers for *in vivo* drug delivery, benefit from easy preparation techniques, acceptable toxicity profiles, and a lack of clearance by the reticuloendothelial system. Liposomes, however, have several drawbacks, including the efficiency of targeting and issues associated with accelerated blood clearance.[18] Although exosomes and liposomes have similar phospholipid bilayers, exosomes consist of only biogenic substances. The potential of exosomes as drug delivery carriers, however, is largely unknown. Adding appropriate targeting molecules can cause exosomes to accumulate at sites of disease *in vivo* (ref. 7 and **Figure 4**). Thus, the biocompatibility and toxicity profiles of exosomes, which notably are natural carriers of miRNA *in vivo*, support their application in drug delivery systems.

To use exosomes clinically, however, further studies are needed to resolve several issues. For instance, therapeutic exosomes should not be quickly cleared by the reticuloendothelial system. In this study, when fluorescently labeled exosomes were injected into the mice tail vein, many exosomes accumulated

© The American Society of Gene & Cell Therapy

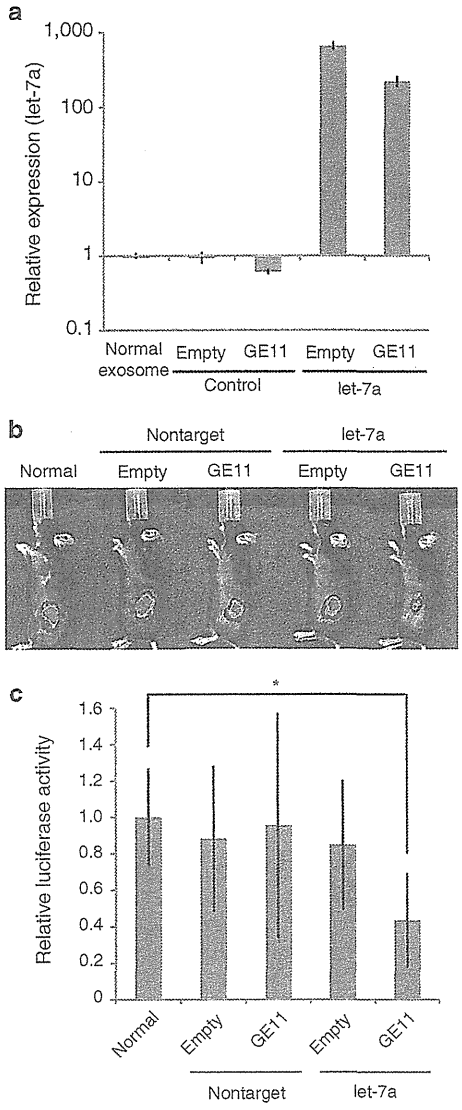

Figure 5 Inhibition of breast cancer development *in vivo* using GE11-positive exosomes containing let-7a. Human embryonic kidney cell line 293 (HEK293) cells expressing GE11 were transfected with synthetic let-7a. Exosomes containing let-7a were purified from culture supernatants and intravenously injected (1 μg of purified exosomes, once per week for 4 weeks) into mice bearing luciferase-expressing HCC70 cells. (**a**) Let-7a levels in the purified exosomes were measured using quantitative PCRs. Data are expressed as means ± SD. $n = 3$. (**b**) Representative images of tumors 4 weeks postinjection are shown. (**c**) Luciferase signals from the tumors were measured using an *in vivo* imaging system (IVIS). Data are expressed as means ± SD. $n = 5$; $^*P < 0.05$.

in the liver 24 hours after the injection (**Figure 4a**). Thus, some modifications are required to avoid normal clearance mechanisms.

This type of delivery strategy requires that the miRNA or siRNA can be efficiently introduced into the exosomes. We transfected donor cells with miRNA and purified exosomes from the culture supernatant. A previous report described electroporation protocols for loading siRNA into exosomes.[8] We, however, were unable to use these methods to load our exosomes with miRNA. The differences in the results may have been caused by the different cell types that were used in the two studies.

The composition of exosomes appears to differ depending on the source tissue or cell type. For instance, major histocompatibility complex class II molecules are enriched in exosomes from B lymphocytes, dendritic cells, mast cells, and intestinal epithelial cells, whereas higher levels of growth factors and their receptors are found in exosomes released from cancer cells.[19] For allogeneic exosome therapy, the presence of major histocompatibility complex proteins is problematic owing to potential immune responses. Therefore, the appropriate selection of donor cells for exosome production is a key factor for potential clinical applications of exosome-based therapies.

In conclusion, exosomes targeted to tumors may allow systemic administration of miRNA as cancer therapy. Technologic improvements that enhance exosome production and reduce immunogenicity should be explored to further develop this drug delivery approach.

MATERIALS AND METHODS

Plasmids transfection and retrovirus infection. The pDisplay vector was purchased from Invitrogen (Carlsbad, CA). Sequence encoding GE11 peptide (YHWYGYTPQNVI) with a flexible peptide linker (GGGGS)3 or mature EGF (53 amino acids, GenBank accession number P01133) was directly fused into pDisplay (**Figure 1a**). HEK293 cells were transfected with pDisplay encoding GE11 or EGF using FuGENE HD transfection reagent (Promega, Madison, WI) and selected with Geneticin (Invitrogen).

EGFR retroviral vector was purchased from Addgene (Cambridge, MA). Viral supernatants were produced by transient transfection of GP2-293T cells with a packaging plasmid (pVSV-G) according to the manufacturer's instructions (Clontech, Mountain View, CA). MCF-7 cells were infected with viral supernatants using polybrene at a final concentration of 8 μg/ml.

Cell culture and small RNA transfection. Breast cancer cell lines (HCC70, HCC1954, and MCF-7) and a HEK293 were purchased from the American Type Culture Collection (Manassas, VA). Cells were cultured according to the manufacturer's instructions. HCC70 cells express firefly luciferase, as previously described.[20] miRNA and siRNA used in this study were as follows: has-let-7a sense (5′-UGAGGUAGUAGGUUGUAUAGUU-3′) and antisense (5′-CUAUACAAUCUACUGUCUUUC-3′); nontarget control miRNA sense (5′-AUCCGCGCGAUAGCACGUAUU-3′) and antisense (5′-UACGUACUAUCGCGCGGAUUU-3′); EGFR-specific siRNA sense (5′-GUGAGGUGGUCCUUGGGAATT-3′) and antisense (5′-UUCCC AAGGACCACCUCACTT-3′); luciferase-specific siRNA sense (5′-CUU ACGCUGAGUACUUCGATT-3′) and antisense (5′-UCGAAGUACUCA GCGUAAGTT-3′); and nontarget control siRNA sense (5′-AUCCGCGC GAUAGCACGUATT-3′) and antisense 5′-UACGUACUAUCGCGCGGA UTT-3′). Oligonucleotides were transfected into cells using HiPerFect reagent (final concentration, 50 nmol/l; Qiagen, Hilden, Germany) according to the manufacturer's instructions.

Western blot analysis. Western blot analysis was performed as previously described.[21] Exosome samples were lysed in sodium dodecyl sulfate loading buffer. After boiling, equal amounts (4 μg) of the proteins were electrophoresed on 15% sodium dodecyl sulfate-polyacrylamide gels and transferred to Immobilon membranes (Millipore, Bedford, MA) using semidry blotting. Then, using standard techniques, the membranes were probed with antibodies, including anti-HA (HA7) (Sigma-Aldrich, St Louis, MO) and anti-HLA-A/B/C (H-300) (Santa Cruz Biotechnology, Santa Cruz, CA). Labeling was visualized using Immobilon Western chemiluminescent

© The American Society of Gene & Cell Therapy

horseradish peroxidase substrate (Millipore) and signals were examined on an LAS-3000 mini system (Fujifilm, Tokyo, Japan).

RNA isolation and quantitative real-time reverse transcription-PCRs. RNA was isolated from exosomes using Isogen reagent (Nippon Gene, Osaka, Japan) according to the manufacturer's instructions. miRNA levels were quantified using TaqMan miRNA assays (Applied Biosystems, Carlsbad, CA). Copy numbers were calculated based on a standard curve created using synthetic RNA. miRNA levels were normalized based on has-miR-16 levels. Quantitative PCRs were run on a Stratagene MX3000P thermocycler and analyzed with MxPro (Agilent Technologies, Santa Clara, CA).

Preparation of exosomes. Exosomes were prepared from HEK293 cells that had been cultured for 48 hours in Dulbecco's modified eagle medium supplemented with 1% GlutaMax (Invitrogen). Cell supernatants were subjected to differential centrifugation. To eliminate cellular debris, samples were centrifuged at 2,000*g* for 20 minutes and 10,000*g* for 30 minutes. Exosomes were pelleted via ultracentrifugation at 120,000*g* for 70 minutes and washed once in phosphate-buffered saline. Protein content in the exosomes was measured using a Protein Assay Rapid Kit (Wako Pure Chemicals, Osaka, Japan). The average exosome yield was 69.2 μg from 100 ml (2–5 × 10^7 cells) of culture supernatant ($n = 8$).

Flow cytometry. For fluorescence-activated cell sorting, exosomes from HEK293 cells were adsorbed onto 4-μm aldehyde-sulphate latex beads (Interfacial Dynamics, Tualatin, OR), incubated with Alexa Fluor 488–conjugated anti-Myc tag antibodies (Millipore, Temecula, CA) or allophycocyanin-conjugated anti-CD81 antibodies (BD Pharmingen, San Jose, CA), and analyzed on a FACSCalibur system (Becton Dickinson, San Diego, CA).

Immunoelectron microscopy. Purified exosomes from HEK293 cells were fixed in 2% paraformaldehyde and loaded onto Formvar-coated Ni electron microscopy grids. The samples were incubated overnight at 4 °C with anti-HA antibodies (Sigma-Aldrich) followed by 1 hour at room temperature with anti-mouse immunoglobulin G conjugated with 15-nm colloidal gold particles. The samples then were fixed in 2% glutaraldehyde, stained with 1% phosphotungstic acid, air-dried, and analyzed using a Hitachi H-7000 electron microscope (Hitachi High-Technologies, Tokyo, Japan). Exosomes positive or negative for gold particles were counted in 10 grids (~1,000–2,000 exosomes).

Coculture of PKH67-labeled exosomes and breast cancer cell lines. Exosomes were stained with green PKH67 fluorescent dye (Sigma-Aldrich). After staining, exosomes were washed with phosphate-buffered saline and centrifuged at 120,000*g* for 70 minutes. One microgram of PKH67-labeled exosomes was incubated with 1 × 10^5 breast cancer cells at 37 °C or 4 °C for 4 hours. The uptake of PKH67-labeled exosomes was analyzed using flow cytometry and confocal fluorescence microscopy.

Administration of let-7a–containing exosomes in a human tumor xenograft model. Luciferase-expressing HCC70 cells (2 × 10^6) were injected subcutaneously into the mammary fat pads of 5-week-old RAG2$^{-/-}$ mice. Four weeks after transplantation, tumors were sized using an IVIS (Xenogen, Hopkinton, MA). HEK293 cells expressing GE11 were transfected with synthetic let-7a. Let-7a–containing exosomes were purified from culture supernatants and intravenously injected (1 μg of purified exosomes, once per week for 4 weeks) into mice with transplanted luciferase-expressing HCC70 cells. Let-7a levels in the exosome samples were evaluated using TaqMan miRNA assays and real-time PCRs. Mice were handled according to the Ethical Guidelines of our institution. All experiments were approved by the Committee for Animal Research at our institution.

In vivo *imaging of fluorescently labeled exosomes.* A stock solution of the lipophilic near-infrared dye XenoLight DiR (Caliper Life Sciences, Hopkinton, MA) was prepared in ethanol. A 300-μmol/l working solution was prepared in diluent-C solution (Sigma-Aldrich). Exosomes isolated from culture supernatant–derived HEK293 cells were incubated with 2 μmol/l DiR for 30 minutes. The exosomes were then washed with 10 ml of phosphate-buffered saline, subjected to ultracentrifugation, and injected intravenously into RAG2$^{-/-}$ mice (4 μg of exosomes/mouse). Migration of fluorescently labeled exosomes in murine organs was detected using an IVIS 24 hours postinjection.

In vivo *imaging of xenograft tumors.* Mice were anesthetized via isoflurane inhalation, and intraperitoneally injected with 100 μl of 7.5 mg/ml luciferin solution (Promega). Bioluminescence imaging was initiated with an IVIS (Xenogen) 10 minutes postinjection. The region of interest was defined manually, and bioluminescence data are expressed as photon flux values (photons/s/cm^2/steradian). Background photon flux was defined using an area of the tumor that did not receive an intraperitoneal injection of luciferin. All bioluminescence data were collected and analyzed using an IVIS.

Statistical analysis. Differences were statistically evaluated using one-way analysis of variance followed by the Fisher protected least significant difference test. P values <0.05 were defined as statistically significant.

SUPPLEMENTARY MATERIAL

Figure S1. Analysis of cell viability based on assays with (4, 5-dimethylthiazol-2-yl) 2,5-diphenyl-tetrazolium bromide.
Figure S2. Hematoxylin and eosin staining of lung, liver, spleen, and kidney tissues from mice injected with exosomes.
Figure S3. Expression analysis of the let-7 target genes.

ACKNOWLEDGMENTS

This work was done in Shinjyu-ku, Tokyo, Japan. This work was supported by the "Private University Strategic Research-Based Support Project: Epigenetics Research Project Aimed at a General Cancer Cure Using Epigenetic Targets" from the Ministry of Education, Culture, Sports, Science and Technology (MEXT) of Japan and in part by a grant-in-aid for scientific research on PriorityAreas (B) and (C) from MEXT (Japan) and the Tokyo Medical University Cancer Research Foundation (Japan). We are also indebted to Roderick J. Turner, Edward F. Barroga, and J. Patrick Barron for their editorial review of the English manuscript. The authors declared no conflict of interest.

REFERENCES

1. Bartel, DP (2004). MicroRNAs: genomics, biogenesis, mechanism, and function. *Cell* **116**: 281–297.
2. Calin, GA and Croce, CM (2006). MicroRNA signatures in human cancers. *Nat Rev Cancer* **6**: 857–866.
3. Barh, D, Malhotra, R, Ravi, B and Sindhurani, P (2010). MicroRNA let-7: an emerging next-generation cancer therapeutic. *Curr Oncol* **17**: 70–80.
4. Lotvall, J and Valadi, H (2007). Cell to cell signalling via exosomes through esRNA. *Cell Adh Migr* **1**: 156–158.
5. Skog, J, Würdinger, T, van Rijn, S, Meijer, DH, Gainche, L, Sena-Esteves, M *et al.* (2008). Glioblastoma microvesicles transport RNA and proteins that promote tumour growth and provide diagnostic biomarkers. *Nat Cell Biol* **10**: 1470–1476.
6. Akao, Y, Iio, A, Itoh, T, Noguchi, S, Itoh, Y, Ohtsuki, Y *et al.* (2011). Microvesicle-mediated RNA molecule delivery system using monocytes/macrophages. *Mol Ther* **19**: 395–399.
7. Kosaka, N, Iguchi, H, Yoshioka, Y, Takeshita, F, Matsuki, Y and Ochiya, T (2010). Secretory mechanisms and intercellular transfer of microRNAs in living cells. *J Biol Chem* **285**: 17442–17452.
8. Alvarez-Erviti, L, Seow, Y, Yin, H, Betts, C, Lakhal, S and Wood, MJ (2011). Delivery of siRNA to the mouse brain by systemic injection of targeted exosomes. *Nat Biotechnol* **29**: 341–345.
9. Woodburn, JR (1999). The epidermal growth factor receptor and its inhibition in cancer therapy. *Pharmacol Ther* **82**: 241–250.
10. Li, Z, Zhao, R, Wu, X, Sun, Y, Yao, M, Li, J *et al.* (2005). Identification and characterization of a novel peptide ligand of epidermal growth factor receptor for targeted delivery of therapeutics. *FASEB J* **19**: 1978–1985.
11. Song, S, Liu, D, Peng, J, Sun, Y, Li, Z, Gu, JR *et al.* (2008). Peptide ligand-mediated liposome distribution and targeting to EGFR expressing tumor in vivo. *Int J Pharm* **363**: 155–161.
12. Klutz, K, Schaffert, D, Willhauck, MJ, Grünwald, GK, Haase, R, Wunderlich, N *et al.* (2011). Epidermal growth factor receptor-targeted (131)I-therapy of liver cancer following systemic delivery of the sodium iodide symporter gene. *Mol Ther* **19**: 676–685.

© The American Society of Gene & Cell Therapy

13. Schäfer, A, Pahnke, A, Schaffert, D, van Weerden, WM, de Ridder, CM, Rödl, W *et al.* (2011). Disconnecting the yin and yang relation of epidermal growth factor receptor (EGFR)-mediated delivery: a fully synthetic, EGFR-targeted gene transfer system avoiding receptor activation. *Hum Gene Ther* **22**: 1463–1473.
14. Takamizawa, J, Konishi, H, Yanagisawa, K, Tomida, S, Osada, H, Endoh, H *et al.* (2004). Reduced expression of the let-7 microRNAs in human lung cancers in association with shortened postoperative survival. *Cancer Res* **64**: 3753–3756.
15. Johnson, CD, Esquela-Kerscher, A, Stefani, G, Byrom, M, Kelnar, K, Ovcharenko, D *et al.* (2007). The let-7 microRNA represses cell proliferation pathways in human cells. *Cancer Res* **67**: 7713–7722.
16. Boyerinas, B, Park, SM, Hau, A, Murmann, AE and Peter, ME (2010). The role of let-7 in cell differentiation and cancer. *Endocr Relat Cancer* **17**: F19–F36.
17. Lee, YS and Dutta, A (2007). The tumor suppressor microRNA let-7 represses the HMGA2 oncogene. *Genes Dev* **21**: 1025–1030.
18. Ishida, T and Kiwada, H (2008). Accelerated blood clearance (ABC) phenomenon upon repeated injection of PEGylated liposomes. *Int J Pharm* **354**: 56–62.
19. Simpson, RJ, Jensen, SS and Lim, JW (2008). Proteomic profiling of exosomes: current perspectives. *Proteomics* **8**: 4083–4099.
20. Murohashi, M, Hinohara, K, Kuroda, M, Isagawa, T, Tsuji, S, Kobayashi, S *et al.* (2010). Gene set enrichment analysis provides insight into novel signalling pathways in breast cancer stem cells. *Br J Cancer* **102**: 206–212.
21. Oikawa, K, Ohbayashi, T, Kiyono, T, Nishi, H, Isaka, K, Umezawa, A *et al.* (2004). Expression of a novel human gene, human wings apart-like (hWAPL), is associated with cervical carcinogenesis and tumor progression. *Cancer Res* **64**: 3545–3549.

連載第7回

新しい消化器疾患動物モデル

消化器発癌モデルマウスを用いた癌エピジェネティクス研究

橋本恭一[1)2)] 波多野裕一郎[3)] 原 明[3)] 坂井義治[2)] 山田泰広[1)]

1) HASHIMOTO Kyoichi, YAMADA Yasuhiro/京都大学 iPS 細胞研究所初期化機構研究部門

2) SAKAI Yoshiharu/京都大学大学院医学研究科消化管外科学

3) HATANO Yuichiro, HARA Akira/岐阜大学大学院医学系研究科腫瘍病理学

Summary

癌細胞には，遺伝子配列の異常が頻繁に観察され，そのような“DNA の傷”が発癌の原因と考えられてきた．一方で，ほぼすべての癌において，遺伝子塩基配列の異常を伴わないエピジェネティック異常が検出される．とくに DNA メチル化修飾状態の異常は，遺伝子発現状態と関連し，発癌に関与していることが明らかになっている．マウスモデルを用いた研究により，エピジェネティック異常の発癌過程における意義が個体レベルで解明されつつある．本稿では，動物モデルを用いておこなわれてきた個体レベルでの癌エピジェネティクス研究を中心に紹介する．とくに家族性大腸腺腫症（FAP）のモデルマウスを用いた実験から明らかとなった，大腸多段階発癌への DNA メチル化の影響について示すとともに，細胞初期化技術を用いた癌エピジェネティクス研究の取り組みについても紹介したい．DNA メチル化異常に代表されるエピジェネティック修飾異常は改変可能であり，癌におけるエピジェネティック制御状態の意義を解明することは，効果的な癌予防および治療方法開発にもつながることが期待されている．

Keywords

大腸発癌，エピジェネティック修飾異常，細胞リプログラミング

はじめに

大腸発癌過程は，病理形態学的に多段階的な変化を経て浸潤癌へと進展する．実際には *de novo* carcinoma のように初期から高悪性度腫瘍である病変も存在するが，多段階の形態変化は，遺伝子変異の蓄積を伴うことが示されており，adenoma-carcinoma sequence や Vogelstein らの提唱した多段階発癌モデルとして広く受け入れられている．現在まで，癌細胞における遺伝子配列異常が多数報告され，おもにリバースジェネティクスの手法により，それらの遺伝子配列異常が癌化の原因となることが，動物モデルを用いて明らかにされてきた．その一方で，DNA 塩基配列異常とは区別されるエピジェネティック修飾異常は，ほぼすべての癌で検出されるものの，その根本的原因は不明であり，その機能的な役割についても不明な点が多い．エピジェネティック制御はクロマチンの構造変化と密接に関連し，発生，分化において遺伝子発現を制御していることが示唆されている．本稿では，いままでにおこなわれた，さまざまなアプローチによるマウス個体を用いた癌のエピジェネティクス研究について紹介したい．

発癌における DNA メチル化異常

ほぼすべての癌細胞において，DNA メチル化，ヒストン修飾に代表される塩基配列異常とは区別される，エピジェネティック修飾異常が観察されている．癌細胞に

おけるエピジェネティック修飾異常のなかでも，DNAメチル化修飾異常が最も盛んに研究されてきた．DNAメチル化パターンは，DNAメチル化維持にかかわるDNA methyltransferase 1（Dnmt1）によりDNA複製の際に維持されるため，癌細胞におけるDNAメチル化修飾異常も遺伝子配列異常と同様に，細胞分裂の際に引き継がれていくことが予想される．したがって，DNAメチル化異常は，遺伝子配列異常と同様に発癌過程で蓄積し，癌細胞が最も増殖しやすいDNAメチル化のパターン異常を有する細胞が選択されていく可能性が考えられている．

癌細胞におけるDNAメチル化異常は大きく分けて2つの特徴がある．癌細胞では，ゲノムワイドにみるとメチル化DNAの総量は低下しているにもかかわらず，特定部位，とくに遺伝子のプロモーター領域に頻繁に分布するCpGアイランドと定義づけられるCG配列が豊富な領域においては高メチル化状態が観察される．おもに培養細胞を用いた研究により，ゲノムワイドなDNA低メチル化状態は，ゲノムの不安定性を引き起こすことで，染色体異常を誘発し，発癌を促進することが示唆されている[1)2)]．実際，DNA複製の際にメチル化パターンの維持を担う*Dnmt1*のノックアウト胚性幹細胞（embryonic stem cell：ES細胞）では，ゲノムワイドな低メチル化状態が観察されるとともに，ゲノムの不安定性を示すことが報告されている[3)]．一方で，部位特異的な高メチル化については，癌抑制遺伝子のプロモーター領域で数多く報告されている．転写開始点近傍の密集したCpG配列でのメチル化の程度と遺伝子発現には強い負の相関があることから，高メチル化状態による癌抑制遺伝子のサイレンシングを介した発癌促進作用が予想されている[4)]．

マウス大腸多段階発癌モデル

われわれは，現在までに動物モデルを用いて大腸発癌メカニズムの解明をめざしてきた．とくに家族性大腸腺腫症（familial adenomatous polyposis：FAP）のモデルマウスである，*Apc*遺伝子に変異を有するMinマウスの大腸発癌メカニズムを分子病理学的に検討してきた．Minマウスの大腸発癌には，肉眼的に確認できない粘膜内の「微小腺腫」と粘膜面に腫瘤を形成する「大腸腫瘤」の少なくとも2段階の過程があることを示し，正常の陰窩上皮から微小腺腫の発生の初期過程に*Apc*遺伝子のヘテロ接合性の消失（loss of heterozygosity：LOH）が関与していることを明らかにしてきた[5)6)]．一方で，粘膜内微小腺腫から大腸腫瘤への進展には，*p53*遺伝子などのVogelsteinらの大腸多段階発癌モデルに示されるような遺伝子に変異は確認されず，このモデルにおける後期進展過程については不明であった[7)]．

*Dnmt1*低発現マウスを用いた癌エピジェネティクス研究

上述のように，DNAメチル化維持にかかわる*Dnmt1*の低発現マウスでは，ゲノムワイドのDNA低メチル化状態が観察される．LairdとJackson-Grusbyら[8)]は，*Dnmt1*ヘテロマウスに脱メチル化剤である5-Aza-2'-deoxycytidineを投与し，強制的にDNAメチル化レベルの低下を引き起こすことで，Minマウスの腸管発癌を抑制することを報告した．この結果は，個体レベルでDNAメチル化が発癌を促進していることを示唆するはじめての報告であり，その後の癌抑制遺伝子におけるDNA高メチル化とサイレンシングの関連性を示す研究を加熱させた[4)9)]．さらには，メチル化DNAとの結合が示されているmethyl-CpG-binding domain protein 2（*MBD2*）のノックアウトマウスでも，腸管発癌が抑制されることが報告され，このことからもDNAメチル化を介した発癌促進作用が示唆された．

このようにして，DNAメチル化による発癌促進作用が注目されていたものの，一方でDNAメチル化レベルの低い*Dnmt1*のノックアウトES細胞では，遺伝子組換えの頻度が増加し，DNAメチル化がゲノムの安定性に寄与し，発癌抑制的に作用していることが示唆されていた．GaudetとEdenら[2)]は，*Dnmt1*低発現アレルを用いて，*Dnmt1*ヘテロマウスよりさらに*Dnmt1*発現量が低いマウスの作製に成功した．ゲノムワイドなDNA低メチル化を示すそのマウスには，T細胞性リンパ腫が自然発生し，neurofibromatosis 1（*Nf1*）；*p53*複合ヘテロマウスの線維肉腫形成を促進することが明らかとなった[1)2)]．T細胞性リンパ腫では染色体数の異常が観察さ